
Masters Theses

Student Theses and Dissertations

Summer 2003

Silica coating of gold nanoparticles

Milind Laxman Surve

Follow this and additional works at: https://scholarsmine.mst.edu/masters_theses

 Part of the [Chemical Engineering Commons](#)

Department:

Recommended Citation

Surve, Milind Laxman, "Silica coating of gold nanoparticles" (2003). *Masters Theses*. 2390.
https://scholarsmine.mst.edu/masters_theses/2390

This thesis is brought to you by Scholars' Mine, a service of the Missouri S&T Library and Learning Resources. This work is protected by U. S. Copyright Law. Unauthorized use including reproduction for redistribution requires the permission of the copyright holder. For more information, please contact scholarsmine@mst.edu.

SILICA COATING OF GOLD NANOPARTICLES

by

MILIND LAXMAN SURVE

A THESIS

Presented to the Faculty of the Graduate School of the

UNIVERSITY OF MISSOURI-ROLLA

In Partial Fulfillment of the Requirements for the Degree

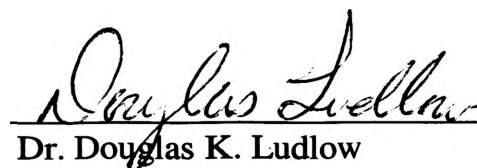
MASTER OF SCIENCE IN CHEMICAL ENGINEERING

2003

Approved by



Dr. Yangchuan Xing, Advisor



Dr. Douglas K. Ludlow



Dr. F. Scott Miller

© 2003

Milind Laxman Surve

All Rights Reserved

ABSTRACT

Gold colloids have been homogeneously coated with silica using silane coupling agents as a primer to make the gold surface vitreophilic. After adding active silica, the particles are transferred in ethanol for uniform silica coating by using the Stöber method. Gold nanoparticles used for this study ranged from 5 nm up to 40 nm with mixed results. Silica condensation can be controlled to produce different silica thicknesses on gold. The main problem while coating smaller particles (5 nm and 10 nm) was the final coagulation or necking of silica after coating the gold surface. The possible causes for this effect are also examined. These composite nanoparticles are then characterized by studying their optical properties particularly absorbance using a fiber optic spectrometer. Such complex but functional particles and structures should have potential applications in optics and other areas.

ACKNOWLEDGMENTS

I would like to express my deepest gratitude to my advisor Dr. Yangchuan Xing for his invaluable guidance throughout the course of this research. I would also like to thank my advisory committee members, Dr. Douglas K. Ludlow and Dr. F. Scott Miller for agreeing to be on my graduate committee. Acknowledgements are also due to Chemical Engineering department of UMR for providing the requisite laboratory space for this research. I would also like to convey my thanks to Intelligent Systems Center for supporting this research.

Last but not least, I would like to thank all my colleagues, instructors, staff members and University of Missouri – Rolla for helping me throughout my graduate work.

TABLE OF CONTENTS

	Page
ABSTRACT	iii
ACKNOWLEDGMENTS.....	iv
LIST OF ILLUSTRATIONS	viii
LIST OF TABLES	x
LIST OF ACRONYMS.....	xi
SECTION	
1. INTRODUCTION	1
1.1. OVERVIEW.....	1
1.2. PROJECT DESCRIPTION.....	2
2. LITERATURE REVIEW	4
2.1. PREPARATION OF SILICA.	4
2.1.1. Reaction Mechanisms	4
2.1.2. Effect of Catalyst.....	6
2.1.3. Silica Gel and Condensed Particles.....	7
2.1.4. Growth Mechanisms of Condensed Silica Particles	8
2.1.5. Stabilization by Silica Shells.....	9
2.2. SYNTHESIS OF GOLD NANOPARTICLES.	11
2.2.1. Turkevich Method.	11
2.2.2. Growth Mechanism	11
2.2.3. Stability of Gold Nanoparticles.	12
2.3. SILANE COUPLING AGENTS.....	13

2.3.1. Amino Organofunctional Trialkoxysilane.....	14
2.3.2. Mercapto Organofunctional Trialkoxysilane.....	16
2.4. ACTIVE SILICA.....	16
2.5. OPTICAL PROPERTIES OF CORE-SHELL PARTICLES.....	18
2.6. ASSEMBLY OF CORE-SHELL NANOPARTICLES.....	21
3. EXPERIMENTAL SECTION.....	23
3.1. GOLD SYNTHESIS	23
3.1.1. Chemical Reagents.	23
3.1.2. Experimental Procedure.....	23
3.2. SILANE COUPLING AGENT COATING.....	24
3.2.1. Chemical Reagents.	24
3.2.2. Experimental Procedure.....	24
3.3. ACTIVE SILICA COATING	25
3.3.1. Chemical Reagents.	25
3.3.2. Experimental Procedure.....	25
3.4. STÖBER METHOD OF SILICA COATING	26
3.4.1. Chemical Reagents.	26
3.4.2. Experimental Procedure.....	26
3.5. ASSEMBLY OF SILICA COATED GOLD NANOPARTICLES	27
3.5.1. Chemical Reagents.	27
3.5.2. Experimental Procedure.....	27
4. RESULTS AND DISCUSSIONS.....	29
4.1. SILICA COATING ON 20 NM GOLD NANOPARTICLES.....	29

4.2. SILICA COATING ON 10 NM GOLD NANOPARTICLES.....	40
4.3. SILICA COATING ON 5 NM GOLD NANOPARTICLES.....	41
4.4. SILICA COATING ON 40 NM GOLD NANOPARTICLES.....	46
4.5. OPTICAL RESULTS OF 20 NM GOLD NANOPARTICLES	47
5. CONCLUSIONS	54
APPENDICES	
A. ABSORPTION SPECTROMETER.....	56
B. TRANSMISSION ELECTRON MICROSCOPE	59
BIBLIOGRAPHY	62
VITA	64

LIST OF ILLUSTRATIONS

Figure	Page
2.1. Variation of hydrolysis reaction rate with pH.....	6
2.2. DLVO total interaction energy-interparticle separation profiles for silica particles in 0.15 M NaCl solution at various pH values	10
2.3. Hydrolyzed 3-APS seven membered ring structure	15
4.1. Bare 20 nm gold nanoparticles prepared by Turkevich Method.....	30
4.2. Active silica coating on 20 nm Au nanoparticle	30
4.3. 5 nm silica coating on 20 nm Au nanoparticles	31
4.4. 10 nm silica coating on 20 nm Au nanoparticles	31
4.5. 20 nm silica coating on 20 nm Au nanoparticles	32
4.6. 30 nm silica coating on 20 nm Au nanoparticles	32
4.7. 10 nm silica coating on 20 nm Au nanoparticles by batchwise TEOS addition	33
4.8. Batchwise silica coating on 20 nm Au for an expected thickness of 80 to 100 nm.....	33
4.9. 10 nm silica coating on 20 nm Au nanoparticles for EtOH/H ₂ O ratio higher than 2.0.....	34
4.10. No silica coating on 20 nm Au for EtOH/H ₂ O ratio less than 2.0	34
4.11. Silica coating on 20 nm Au nanoparticles without any pre-coating with 3-APS and/or active silica... ..	35
4.12. Coating on 15 nm Au nanoparticle after five APS layers of precoating.....	38
4.13. Coating on 15 nm Au after ten APS layers of precoating.....	38
4.14. Silica coating on 15 nm Au when TEOS is added in a semibatch way	38
4.15. Heating effect on the silica coating of 20 nm Au particle.....	38
4.16. Silica coating on 20 nm Au for lower ammonia concentration.....	39

4.17. Silica coating on 20 nm Au for higher ammonia concentration	39
4.18. Gelling due to direct contact of acid with sodium silicate while preparing active silica	40
4.19. Silica coating on 10 nm Au for EtOH/H ₂ O ratio of 7.5	41
4.20. Silica coating on 10 nm Au for EtOH/H ₂ O ratio of 12	41
4.21. Silica coating on 5 nm Au for TEOS=192 μM and NH ₃ =0.212 M.....	43
4.22. Silica coating on 5 nm Au for TEOS=3.06 mM and NH ₃ =0.212 M.....	43
4.23. Silica coating on 5 nm Au for TEOS=756 μM and NH ₃ =0.417 M.....	43
4.24. Effect of ethanol dilution on coagulation of silica coated 5 nm particles	43
4.25. Effect of higher dilution on coagulation of silica coated 5 nm gold nanoparticles.	45
4.26. Initial addition of ethanol for complete condensation of active silica	45
4.27. Effect of grid heating to prevent coagulation of silica while drying the grid	46
4.28. Silica coating on 40 nm Au nanoparticle	47
4.29. Optical spectra of Bare Au	48
4.30. Optical spectra of Au coated by 3-APS	49
4.31. Optical spectra of Au coated by 5 nm silica.....	50
4.32. Optical spectra of Au coated by 10 nm silica.....	51
4.33. Optical spectra of Au coated by 20 nm silica.....	51
4.34. Optical spectra of Au coated by 30 nm silica.....	52
4.35. Normalized solution absorbance spectra of 20 nm Au compared with 3-APS and various thickness of silica.....	52
4.36. Variation of peak position with different thicknesses of silica	53

LIST OF TABLES

Table	Page
3.1. Dependence of 3-APS or 3-MPTS concentration on gold size.....	25
4.1. Characteristics of different sized Au particles	36

LIST OF ACRONYMS

Symbol	Description
LBL	layer-by-layer
TEOS	Tetraethoxysilane
DLVO	Derjaguin Landau Verwey Overbeek
3-APS	3-Aminopropyl tri-methoxy silane
3-MPTS	3-Mercaptopropyl tri-methoxy silane
Au @ SiO ₂	core material is gold @ shell material is silica
PDDA	Poly (diallyl dimethylammonium chloride)
w.t.%	weight%
TEM	Transmission electron microscope
UV	Ultra violet

1. INTRODUCTION

1.1. OVERVIEW

Modern nanomaterial science has evolved within a few decades [1]. This has been possible due to the various research programs undertaken to develop nanoparticles that have innovative and complex structures. This trend is followed in assembling such particles to form functional structures. In this regard, nanoparticles with core-shell morphologies represent a new type of constructional unit consisting of two dissimilar compositional and structural domains [2]. Such materials should have enhanced physical and chemical properties and a broader range of applications than their single-component counterparts. The properties that are most widely studied are electrical, magnetic or optical. The core-shell particles have different combinations within metal, dielectric and semiconductor materials, for example, Gold (metal core)-Silver (metal shell) or Silica (dielectric core)-Gold (metal shell) or even Cadmium-Selenide (semiconductor core)-Silica (dielectric shell) and so on [3]. The term particle engineering is often used to refer such core-shell particle synthesis [3]. Particle engineering is carried out for various reasons. The shell can enhance the dispersibility and stability of the colloidal core or can alter the charge. Magnetic, optical or catalytic functions of the core nanoparticle can be readily adjusted to desired values by using different shell materials [2]. Encasing colloids in the shell of different compositions can also protect the core from any chemical and physical changes that usually occur in processing conditions [2].

The major challenge for such particle engineering is the precision sought in coating the core nanoparticles. Although varieties of procedures are used to produce such composite structures, difficulties associated with their production have limited their final

application. Some of the processes used are solution chemistry, membrane-based synthesis, layer-by-layer (LBL) method, gas synthesis etc. [1]. The final application of the core-shell particles dictates the synthesis process to be used. All of these processes fulfill the major requirements of such core-shell particles. Some of these requirements are monodispersed size, stable in most solvents (polar or non-polar), uniform charge distribution on the shell surface, fairly concentrated mixtures of core-shell particles, easily assembled to form functional structures and lastly easy characterization for desired properties.

1.2. PROJECT DESCRIPTION

The project deals with the synthesis and characterization of gold-silica core-shell nanoparticles. It uses solution chemistry to polymerize silica on gold surface and form a coating of desirable thickness. This surface reaction (Stöber method) is the hydrolysis and condensation of TEOS (Tetraethoxysilane) in the presence of ammonia as a morphological catalyst [4]. This method was found useful for particles of gold down to 15 nm. However, this research specifically deals with coating gold nanoparticles of size less than 15 nm, like 10 nm, 5 nm and 2 nm. The coating of such smaller gold particles is desired because the properties of nanoparticles depend on size. Hence, it is expected that these core-shell particles would have different properties than larger coated gold nanoparticles. In addition, modern nanotechnology demands smaller particles for higher density functional structures. The property of significance for this project is the optical properties of both gold and silica coated gold particles. Gold has a typical plasmon absorption peak around 520 nm [5], which after silica coating gets red-shifted, i.e. shifts

to higher wavelength. The main difficulty with gold-silica core-shell particle synthesis is the lack of chemical affinity between gold and silica. This means that some procedure has to be identified to overcome the low tendency of the gold and silica to bond together. Liz-Marzán et al. [6] tried to overcome this shortcoming by coating gold nanoparticles by the Stöber method. This method produced labeled and unlabelled silica particles with higher percentage of unlabelled ones. A higher proportion of labeled silica particles was accomplished by Liz-Marzán et al. [5] by first coating the gold surface by a bi-functional silane coupling agent (3-Aminopropyl trimethoxysilane) followed by final silica coating using the same Stöber method. However, they used 15 nm gold colloids for their experiments, for which they got mono-dispersed silica coating up to 80 nm thickness with very high homogenous nucleation.

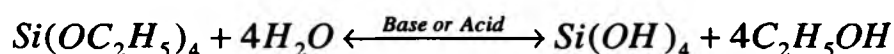
Thus, the process of silica coating would be based on Liz-Marzán method except that the objective would be to have smaller gold particles coated and assembled to form films. These composite particles and films are characterized by checking their optical properties.

2. LITERATURE REVIEW

2.1. PREPARATION OF SILICA

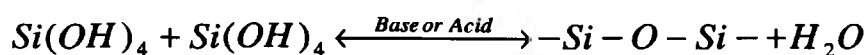
Silica is produced by using the Stöber method [4] which is the hydrolysis and condensation of TEOS in the presence of ammonia as a morphological catalyst. This is further described in the following sub-sections.

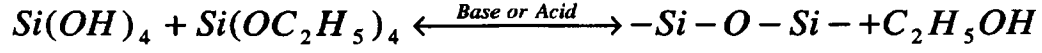
2.1.1. Reaction Mechanisms. TEOS is a type of alkoxy silane which is the most commonly used precursor for silica coating. Hydrolysis is the first reaction where TEOS reacts with water. This reaction takes place by nucleophilic attack of the oxygen contained in water on the silicon atom of TEOS. The mechanism of this reaction is [7,8,9].



Reaction rate of hydrolysis increases by using either acid or base. The most common acid used is hydrochloric acid while the most common base used is ammonia. Hydrolysis is facilitated in the presence of homogenizing an agent such as alcohols. It should be emphasized that the addition of solvents may promote esterification i.e. the reverse of the above reaction. Although hydrolysis in alkaline environments is slow, it tends to be complete and irreversible [7].

In condensation or polymerization reaction, siloxane bonds forms by either alcohol or water producing reaction. In this reaction, monomer (i.e. TEOS without any ethyl groups) or dimer, trimer, cyclic trimer, cyclic tetramer, higher order rings or even TEOS condenses. The mechanism of this reaction is as given below.





The reversibility of the condensation depends on the pH and solvent used. Overall, the reaction is fast compared to hydrolysis since the reaction reaches equilibrium very rapidly and the intermediates formed have a very short active life. The effect of catalyst or pH on the rate of condensation is the same as for hydrolysis.

Chen et al. [10] performed experiments to evaluate the kinetic constant equations for hydrolysis and condensation reactions of TEOS. Their empirical equations show that the kinetic constant depends on temperature, water, and ammonia concentration. The hydrolysis of TEOS was found to be first order with respect to TEOS, being consistent with previous works. Thus, plot of $\ln ([TEOS]_0 / [TEOS])$ versus reaction time t shows a linear dependency. The silicic acid condensation was also found to be first order with respect to silicic acid; the first order rate constant of TEOS hydrolysis and silicic acid condensation are as given below.

Assume K_h and K_c is functions of temperature T , $[H_2O]$, and $[NH_3]$ as follows:

$$K = K_0 \exp\left(-\frac{E_a}{RT}\right) [H_2O]^\alpha [NH_3]^\beta \quad (1)$$

and the empirically found rate constants are as follows:

$$K_h = 74.36 \exp\left(-\frac{E_a}{RT}\right) [H_2O]^{1.267} [NH_3]^{0.971} \quad (2)$$

where, $E_a = 25.2$ kJ/mol

$$K_c = 19408 \exp\left(-\frac{E_a}{RT}\right) [\text{H}_2\text{O}]^{1.196} [\text{NH}_3]^{0.7854} \quad (3)$$

where, $E_a = 33.2$ kJ/mol

2.1.2. Effect of Catalyst. Brinker et al. [7] has studied the hydrolysis of TEOS in buffered aqueous solution. They inferred from hydrolysis rate constants plotted against pH that the minimum rate was around pH 7 while both acidic and basic conditions increased the rate of hydrolysis as shown below in Figure 2.1. Under acidic conditions, it is likely that an ethoxide group is protonated in a rapid first step. This withdraws the electron density from the silicon atom making it more electrophilic and thus more susceptible to attack from water. Base catalyzed hydrolysis of TEOS is slower than acid at an equivalent catalyst concentration. This is because the basic ethoxide oxygen tends to repel the nucleophilic hydroxyl ion.

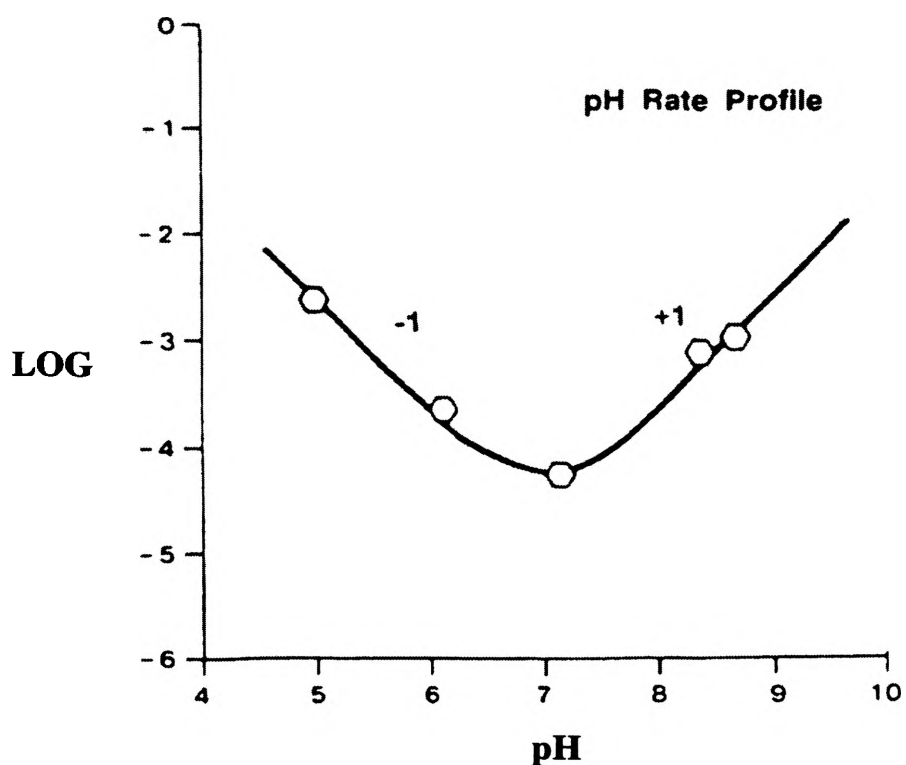


Figure 2.1. Variation of hydrolysis reaction rate with pH. From [7].

However, once an initial hydrolysis has occurred, the reactions proceed stepwise with each subsequent ethoxide group easily removed from the monomer than the previous one. As said earlier, the effect of catalyst (acid or base) on condensation reaction is same as that for hydrolysis.

2.1.3. Silica Gel and Condensed Particles. When acid like hydrochloric acid is used for TEOS hydrolysis and condensation, the final silica formed has physical features of gel. Usually this gel network has poor branched network of silica monomers to form a lower molecular weight polymer. This low molecular weight structure is partly due to the irreversibility of the condensation reaction. This irreversibility causes depletion of monomers as all of them are consumed by condensation reaction. The resulting clusters are unable to interpenetrate and condense to completely fill the space due to steric and kinetic constraints. Such gel is characterized by a mass fractal dimension (D) of 2.05.

While in base catalyzed hydrolysis and condensation of TEOS, the reversibility of the condensation favors a three-dimensional molecular network of condensed silica. The reversibility or depolymerization hydrolyzes the siloxane bond formed during condensation and thus insures reaction limited conditions. Depolymerization occurs preferentially at less stable sites and therefore repeated depolymerization / repolymerization forms stable (i.e. lower surface energy) configuration at the expense of unstable ones. Gelation is not observed because after the particles have reached a certain size (after continuous rearrangement) they are electrostatically stabilized and hence mutually repulsive. Such condensed silica particles have a characteristic mass fractal dimension (D) of 3.

2.1.4. Growth Mechanisms of Condensed Silica Particles. The structural evolution of condensed silica particles follows the generally accepted model in aqueous media that is nucleation and growth. As the supersaturation is achieved, a short burst of nucleation occurs whereby the monomers are formed into nuclei. This is followed by self-sharpening mechanism where nuclei grow by the addition of more monomers. This continuous growth of the nuclei causes it to go beyond solubility equilibrium causing it to precipitate from the solution. This growth mechanism, called the LaMer model [9] is surface reaction limited as it depends on the monomer formed during condensation reaction.

Bogush et al. [11,12] has proposed a different growth model that of silica nuclei aggregating to form particles until they reach a size where aggregation no longer occurs. This mechanism proceeds independently of the presence of particles. The main assumptions of this model are that the particles grow solely by binary aggregation, aggregating particles coalesce to form a spherical particle, nucleation produces primary particles of constant size at a rate that relates to the loss of soluble species from solution and aggregation rates are determined by typical colloidal interaction potentials. Thus, unless stabilized by a repulsive force substantially stronger than electrostatic repulsion, small primary particles would aggregate. Hence, as the particle size increases, the barrier to aggregation also increases due to higher surface potential.

Bogush et al. proved that aggregation model was a better mechanism than LaMer model because, when NaCl is used as an electrolyte, the particle size of the condensed silica particle increased without changing the reaction rate. This showed that though the reaction rates were same for both ionic and non-ionic condensation, the final particle size

distributions were not. This totally contradicts the LaMer model. However, the aggregation model also has limitations since it predicts the fractal dimension to be less than 3 and porosity higher than normally expected for such particles. Hence, aggregation model is simply an extension of the LaMer model to the case where nuclei may be colloidally unstable. Thus, he concluded that aggregation is unlikely to be the only step in the formation of all uniform precipitates; colloidal interactions clearly, play a key role in determining the particle size distribution along with surface reaction mechanism.

2.1.5. Stabilization by Silica Shells. One of the great advantages of core-shell particle geometry is that the shell material solely determines its stability. To explain the reasons why the encapsulation of various nanoparticles with silica enhances their colloidal stability, the basic colloidal stability of silica sols is studied. Van der Waals force is the dominant force when two particles approach each other. This force neutralizes only if the silica shell thickness is well above 1 nm. Silica has extraordinary stability against coagulation. Contrary to DLVO (Derjaguin Landau Verwey Overbeek) theory, it has been observed that silica sols in the size range of 10-100 nm possess a remarkable stability at very high salt concentration (e.g., 0.15 M NaCl) at $\text{pH} \geq 10.5$, and even at their isoelectric point (pH_{iep} which is around 2). This stability is due to silica's lower Hamaker constant as compared to other metals, latex or oxide particles.

Stability of silica particles depends on the solution pH. The DLVO theory predicts that a 15 nm silica sol will coagulate at $\text{pH} \geq 11$ and 0.15 M NaCl, as illustrated by the curves of interaction energy (V_{T}) of two identical silica spheres approaching one another. Figure 2.2 demonstrates that at this ionic strength the Van der Waals interaction dominates at all separations for all pH values. Also, from the plot it is seen that as the

surface charge decreases with decreasing pH, the primary minimum of V_T will deepen and hence coagulation will occur rapidly. Contrary to this theory, Iler [13] has noted that silica sols are stable at near neutral pH and at pH_{iep} . Allen and Matijevic [12] also observed the same phenomenon for 15 nm diameter Ludox silica particles that were stable in the pH range of $pH_{iep} - pH 10$ at 0.15 M NaCl. The contradiction to the DLVO theory can be because of its limiting applicability to such smaller particles. They also observed that below pH 11, the critical coagulation concentration (c.c.c.) of NaCl increased as the pH decreased. For instance, even at pH 7, Ludox silica sols were stable at 1.5 M NaCl.

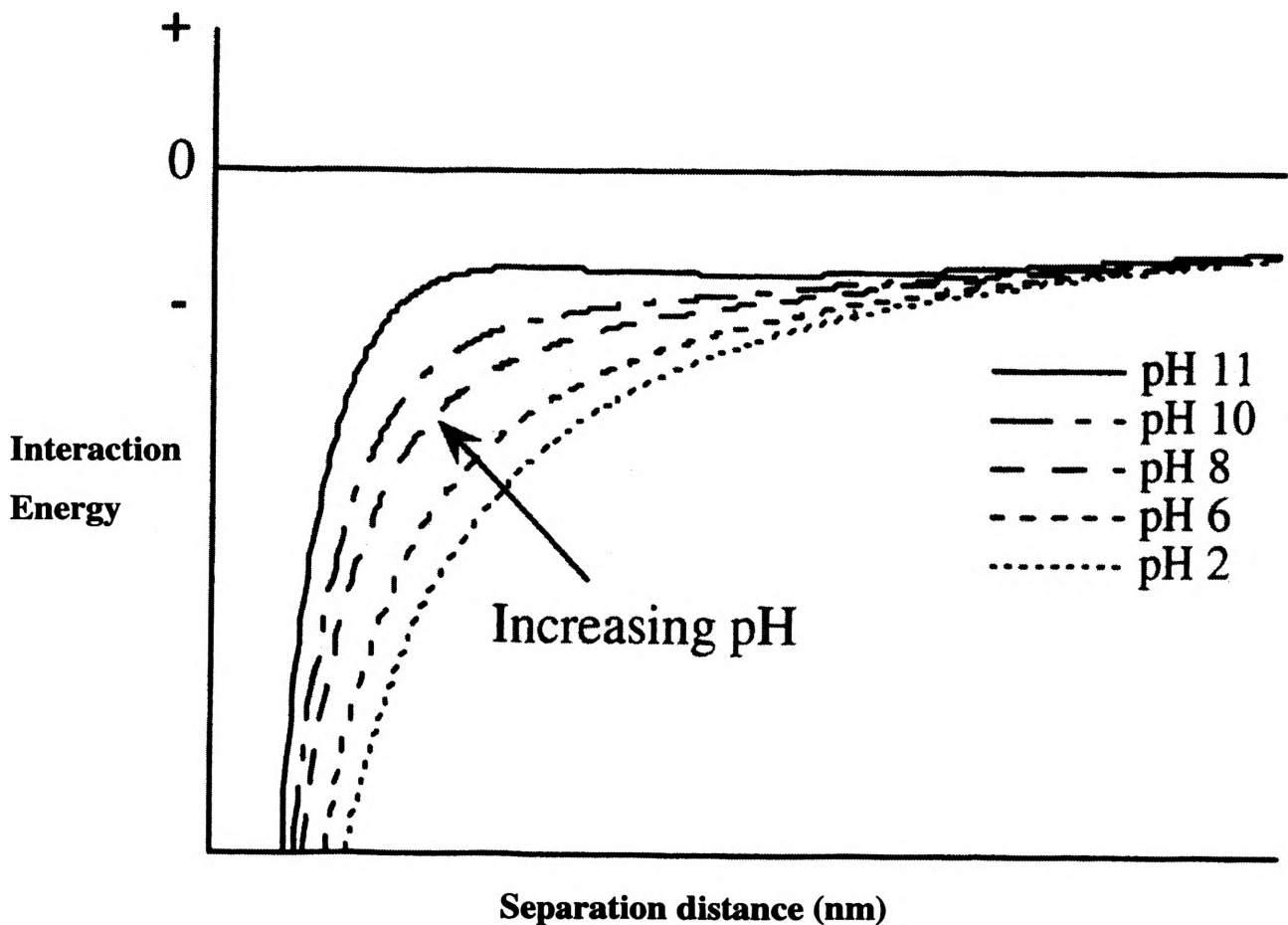


Figure 2.2. DLVO total interaction energy-interparticle separation profiles for silica particles in 0.15 M NaCl solution at various pH values. From [3].

2.2. SYNTHESIS OF GOLD NANOPARTICLES

Gold nanoparticles are one of the oldest colloidal particles prepared. Faraday was first to come up with a simple method for preparation of gold sol using reduction of chloroauric acid solution by phosphorous-ether solution. The following sections deals with the synthesis, growth mechanism and stability of these gold particles.

2.2.1. Turkevich Method. Turkevich et al. [15] has successfully prepared monodispersed gold nanoparticles of diameter down to 12 nm. The method uses sodium citrate as a reducing agent to reduce boiling chloroauric acid aqueous solution. The ratio of sodium citrate to chloroauric acid used for this procedure is around 5:1 to form monodispersed particles. It takes about 10 minutes to form the red colored gold colloidal sol. gold nanoparticles formed by this method has a polycrystalline structure. Other reducing agents used were acetone, tannin, oxalic acid, hydroxylamine, carbon monoxide, acetylene and citric acid. However, only with sodium citrate were the gold particles monodispersed and relatively smaller in size. These particles have high stability and don't aggregate up to 10 days. This stability is primarily due to the negative citrate ions in the solution. These ions increase the repulsion barrier and prevents aggregation.

2.2.2. Growth Mechanism. Gold nanoparticles formed by the Turkevich method has spherical shape as it is the minimum energy state. For silica coating, spherical, cubical or some other compact shape gold nanoparticle is preferred. The chemical reduction always proceeds in a fast and uncontrollable manner.

Leontidis et al. [16] has observed that irregular aggregates formed initially are in the order of 50 nm or larger. This bigger aggregate consists of much smaller individual gold nuclei of around 5 nm. These nuclei grow by simultaneous process of sintering and

nuclei addition on their surface. The narrow size distribution is due to the rapid initial burst of nucleation followed by relatively slow surface growth. The gold nuclei after sufficient surface growth reach equilibrium and stops growing. The citrate ions used for reducing are in excess amount to prevent gold aggregation at this concentration. The excess citrate surrounds the gold particles and increases the repulsion barrier for stability.

2.2.3. Stability of Gold Nanoparticles. In a solution, there are various forces acting on colloidal particles that dictate the stability and thermodynamic behavior. The forces normally acting are double-layer repulsion, Van der Waals forces, Steric forces etc. The double layer repulsion originates from the distribution of both counter ions and co-ions close to the charged particle surface. This layer consists of two regions, Stern layer and diffuse layer. The cause of particle surface charge is due to solution pH, adsorbed ions or polyelectrolytes, preferential dissolution of lattice ions and electronic charge. Ionizable molecules or polyelectrolytes normally stabilize metal particles like gold. Van der Waals force consists of dispersion and London forces. This force is responsible for attraction between any type of atoms and molecules whether charged or neutral. They are also present in the interaction between particles in any suspension medium. DLVO theory is used to calculate the total interaction potential i.e. sums of repulsion and attractive forces from double layer repulsion and Van der Waals force, respectively.

Polyelectrolyte polymers produce steric forces when adsorbed on particle surface. Gold nanoparticles do not exhibit steric forces, as it is normally present in solvents with high enough dielectric constant (ϵ_r). The main problem with gold nanoparticle dispersions is its lower stability in ethanol solutions as compared to that in aqueous solutions. The

solvent polarity and dispersion constant decreases from water to ethanol (ϵ_r (water) is 78.5 and ϵ_r (ethanol) is 25). Thus, transferring from water to ethanol is equivalent to decrease in potential from -78.5 to -25 mV [3].

2.3. SILANE COUPLING AGENTS

Silane coupling agents are hybrids of silica and of organic materials related to polymers or resins; hence, it is not surprising that they are used as coupling agents to improve bonding of organic polymers or resins to mineral surfaces. They normally function as (1) a finish or surface modifier (2) a primer (3) an adhesive, depending on the thickness of the bonding material at the interface [17].

Before applying to the surface, these silane agents are hydrolyzed with water. This requires understanding of their reactions both with and in water. After hydrolyzing, it further condenses to form oligomeric siloxanols. The hydrolysis and condensation kinetics of the silane agents were reported by Pohl and it follows the same mechanism as alkoxy silane as discussed earlier. In addition, the kinetic rate has the same dependency on acid and base catalysts as alkoxy silane. The solubility of these silane compounds generally depends on the type of solvent used and whether the functional group is neutral, cationic or anionic. As they are condensed after hydrolysis, the solubility starts to decrease due to increase in molecular weight. However, it should be noted that decrease in solubility should not cause haze formation in the solution as it loses its usefulness.

Some silane coupling agents used are 3-Aminopropyl tri-methoxy silane (3-APS), 3-Mercapto propyl tri-methoxy silane (3-MPTS), 3-Glycidoxypropyl tri-methoxy silane (3-GPS), 3-Methacryloxypropyl tri-methoxy silane (3-MPS), etc. All these silane

coupling agents are bi-functional i.e. MPTS has two different functionality components i.e. $-SH$ (mercapto group) and $-Si-(OCH_3)$ (silane group). For gold nanoparticles, both MPTS and APS can be used. This is because both these compounds have functional groups that have an affinity towards gold surface. APS has $-NH_2$ (amine group) and MPTS has $-SH$ (mercapto group) [5,18]. Thus, by having either of these silane coupling agents on it makes gold surface vitreophilic i.e. conditions the gold for further silica coating through the siloxane bonds ($-Si-O-Si-$) which are formed through the other end of the coupling agent. As amino and mercapto organofunctional trialkoxysilanes are mostly used coupling agents for making the gold surface vitreophilic, they are discussed in detail in the following sections.

2.3.1. Amino Organofunctional Trialkoxysilanes. This type of silane has cationic amine group as one of its functional group. This amine is hydrophilic and has strong affinity towards gold surface. 3-APS is one of such amino trialkoxysilanes commercially available. The alkoxy group attached to silicon for this chemical is methoxy that can also be replaced by ethoxy with no difference in its applicability.

This type of silane hydrolyzes immediately at alkaline pH. After hydrolysis, it remains stable in water at all concentrations due to the strong hydrophilic nature of its organo functional group. The cationic NH_2^+ group has strong affinity for gold surface. These types of silanes are different from neutral organo functional silanes that are not stable even at moderate concentrations in aqueous solutions. It is proposed that the unique solubility of such trialkoxysilane is due to the internal cyclization between nitrogen and silicon or silanolate ion. By using the analogy of Frye et al. [17] penta-coordinate bridgehead structure of siloxazoladines, the hydrolysis structure of amino

trialkoxysilanes can too be expected to be penta-coordinate one. However, ^1H NMR or Fourier transform IR techniques do not show such a penta-coordinate structure. It shows a structure as an internal bonded seven membered ring. Chiang et al. [17] has shown three possible conformations for hydrolyzed 3-APS. One of the conformations that are most likely to occur is as shown in Figure 2.3 below. This structure is consistent with the chemistry of amino trialkoxysilane. Bonding of amine hydrogen explains the lack of activity of amino propyl silanes in alcoholic solvents while that of silanol hydrogen explains the stability against cross-linking of tri-functional amino alkylsilanes in relatively concentrated solutions.

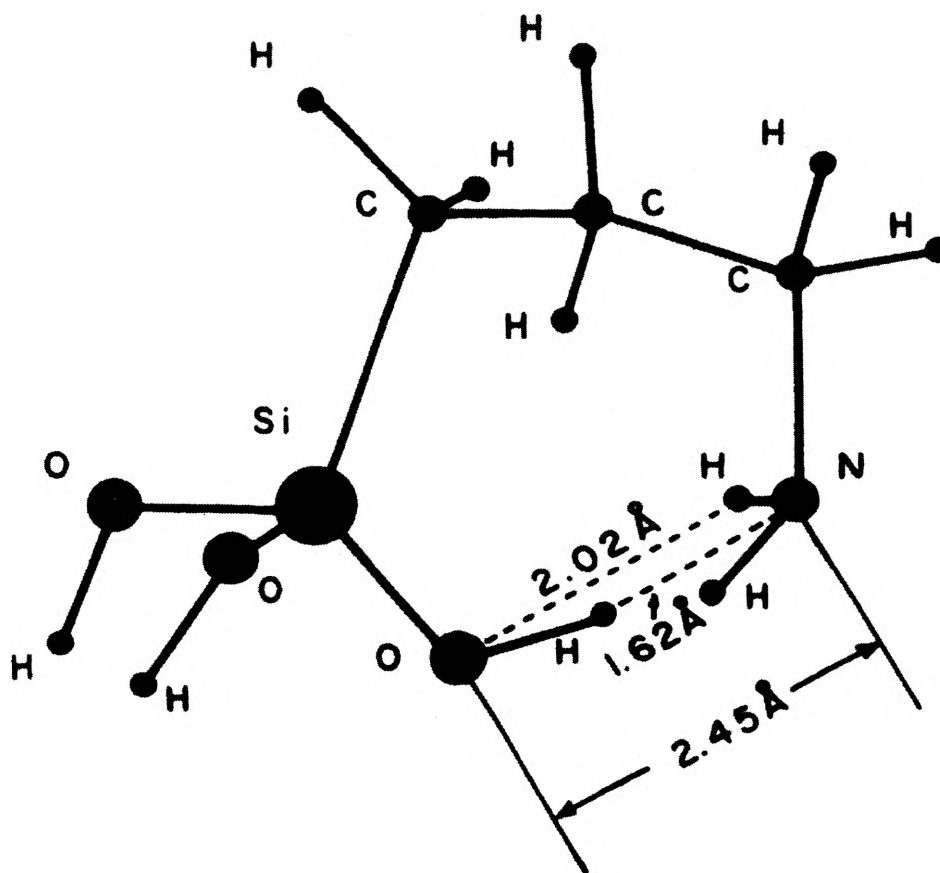


Figure 2.3. Hydrolyzed 3-APS seven membered ring structure. From [17].

2.3.2. Mercapto Organofunctional Trialkoxysilanes. This type of trialkoxysilane also has a cationic functional group i.e. mercapto SH^+ group. The mercapto group is less hydrophilic than amine group. 3-MPTS is one of the commercially available mercapto trialkoxysilane. The stability of mercapto trialkoxysilane is low as compared to amino trialkoxysilane in aqueous solutions but in alcohols, it is much better than amino trialkoxysilane. This low stability could be because of the absence of the hydrogen-bonded ring like structure observed for amino trialkoxysilane. The mercapto group has same affinity as amine group towards gold surface.

2.4. ACTIVE SILICA

Active silica is a type of highly reactive colloidal solution of silicon dioxide. Though there are various methods by which silicon dioxide solution can be prepared, the most efficient method is that of Bird [19]. This method is an improvement of previous processes and forms highly reactive colloidal solution of inorganic oxides in general. The underlying principle upon which the method is based is the passage of any alkali compound of an element over an acid-regenerated zeolite or exchange material whereby the alkali is substantially removed from the compound, leaving the oxide of the element in solution in the colloidal state. This highly reactive colloidal solution is used for silica coating of any vitreophilic surface and is usually done in an aqueous environment.

Silica (silicon dioxide, SiO_2) can be prepared by passing or contacting sodium silicate ($\text{Na}_2\text{Si}_3\text{O}_7$) solution with a mass of acid-regenerated zeolite that results in the adsorption of the sodium ion from the sodium silicate by the zeolite and which yields a colloidal solution of silicon dioxide. When the zeolite or the exchange materials have

adsorbed its full quota of alkali, it can be restored or regenerated by passing an acid solution over it. This forms a soluble alkali compound that may then be washed from the exchange material by water and the regenerated zeolite may be employed for treating new amounts of the alkali compound of the said element or other analogous compounds.

The commercially available sodium silicate solution has the ratio of SiO_2 to Na_2O (stoichiometrically determined) of around 3.0 and SiO_2 content around 30 w.t.%. A dilute solution (around 10 w.t.% of SiO_2) prepared from this available concentrated sodium silicate does not change the SiO_2 to Na_2O ratio but after the above treatment with acid regenerated zeolite causes the ratio to change from 10:1 to 100:1. However, a 50:1 ratio is preferable for normal application of silica coating of a surface with small residuary amount of sodium metal to prevent gelling of the formed silica. Even the SiO_2 content should not be larger than 10 w.t.% to prevent gelling. This colloidal solution is a mixture of very small insoluble silica particles (size less than 1 nm) and soluble silica in a reactive form. This silica when in contact with a vitreophilic surface starts to deposit and polymerize simultaneously if the pH of the solution is from 8 to 11. According to Iler, this pH range is necessary for condensed silica coating. The polymerized silica formed in this process is rough i.e. very porous in nature and is a very slow process. Hence, it takes at least a day to form an appreciable layer on the surface. However, this process can be speeded up by moderately heating the colloidal solution to around 60°C . This heating also increases the molecular weight of silica.

The zeolite or exchange mass that is normally used is a cationic exchange resin having Na^+ as the cation on it. This resin is synthetically prepared rather than made of wood or such cellulosic material. Thus, when acid is passed over it, the sodium forms its

salt (such as NaCl, Na₂SO₄, etc.) and H⁺ ions gets on the resin making it active for further treatment. This acid regenerated resin contacts with sodium silicate, it exchanges Na⁺ for H⁺ on the resin and hence forms silicon dioxide or silica. This process can be repeated until the desired ratio of SiO₂:Na₂O is achieved. While after the resin is saturated, the Na⁺ on the exhausted resin can again be replaced by H⁺ ions by treating with acid again i.e. repeating the previous step again. The contact of the resin and sodium silicate can be done either in an exchange column or in a simple beaker with stirring. The only problem with exchange column is that sometimes due to the acidic pockets in the column, the silica gels and hardens. This causes blocking of the smooth passage of the silicate solution and hence hampers the whole process.

2.5. OPTICAL PROPERTIES OF CORE-SHELL PARTICLES

The optical behavior of nanoparticles can be explained by Mie theory for light absorption and scattering after combining it with the classical Drude model for estimating the dielectric properties of metals [3]. The mechanism for the absorption of light by small metal particles is based on the theory that the plasma oscillation of the conduction electrons of the particle is caused by the restoring force resulting from the induced charge separation on the surface of the particle during the interaction between the electromagnetic field and the particle. This absorption in UV-visible region by metal particles is sensitive to particle size, shape, solvent medium, chemical composition of particle and shell material, electron density on the particles and temperature. Mie theory states that the absorbance, A , of light occurs as the irradiance of a beam of light is

exponentially attenuated from I_0 to I_t in traversing a distance through a dilute solution containing N particles per unit volume,

$$A = -\log_{10}\left(\frac{I_t}{I_0}\right) = \frac{NC_{ext}l}{2.303} \quad (4)$$

where C_{ext} is the extinction cross section of a single particle, which results from both scattering and absorption of light by particle. Though both scattering and absorption occur simultaneously, most of the time one dominates the other. For example, for metal nanoparticles as small as 20 nm, absorption dominates scattering. Hence, absorption is given much more importance than scattering for such smaller particles. Mie theory only deals with absorbance of a pure metal particle but it can be modified to estimate the absorption properties of core-shell particles too. In such cases, the dielectric function and the volume fraction of the coating material should be considered in addition to the dielectric function of the surrounding medium.

Au @ SiO₂ (it means core-material @ shell-material) nanoparticles constitutes a perfect model system for testing the applicability of Mie theory since gold has a strong plasmon absorption band while silica is electronically inert. Thus, silica does not exchange charge with the gold cores. Therefore, there is no risk of electronic interactions that could affect the optical properties as happens in the case of some metal @ metal systems. The extinction coefficients of Au @ SiO₂ particles have been calculated systematically as a function of shell thickness and solvent refractive index using the modified Mie theory. After comparing it with the experimental spectra, it shows a slight mismatch due to the limited accuracy with which the dielectric function of the bulk metal

can be determined. The main effect of this discrepancy is that the experimental peak positions are systematically observed to be at shorter wavelengths than as predicted using Mie theory.

The influence of the silica layer on the optical properties of the colloid is that as the shell thickness increases, there is an increase in the intensity of the plasmon absorption band, as well as a red shift (i.e. shift to longer wavelengths) in the position of the absorption maximum. This is due to the increase in the local refractive index around the particles. However, when the silica shell is sufficiently thick, scattering becomes significant, resulting in a strong increase in the absorbance at shorter wavelengths. This effect causes the peak to be blue shifted to shorter wavelengths due to the scattering effect. At around 80 nm shell thickness, scattering totally masks absorption phenomenon. In addition, a plot of experimental peak positions against silica shell shows the same trend as Mie theory except that due to the presence of gold-free silica particles, the scattering observed practically is high enough. This causes the theoretical estimates to increase larger values than actually observed. Scattering effect can be decreased dramatically by matching optical index of silica by choosing the proper solvent.

Silica coating also allows a detailed investigation of the effect of temperature on the plasmon band of gold particles as heating causes gold aggregation. When extinction intensity around gold plasmon band (500 to 550 nm) is compared with temperature, it is seen that it steadily decreases with increasing temperature [3]. There are four possible contributions to this behavior: metal expansion, solvent refractive index changes, solvent expansion, and resistivity changes in the metal as a function of temperature. Out of these factors, both resistance changes and solvent expansion appear to be the most important

ones while others have much smaller effect. In all these calculations, the main assumption is that there is no effect of temperature on the silica shell.

2.6. ASSEMBLY OF CORE-SHELL NANOPARTICLES

One of the most important applications of metal and semiconductor nanoparticles is the formation of nanostructured functional structures. Silica in colloidal form can be used to form two-dimensional and three-dimensional functional structures. Silica coated nanoparticles are found to be more useful to form structured materials as compared to surfactant stabilized particles. This is because surfactant or polymer stabilized particles have limited thickness, chain melting, and chemical oxidation that all conspire to limit flexibility and application. In addition, silica coated materials open much more options for forming 2-D and 3-D structures due to the possibility of finer surface modification and variation of the thickness of the silica shell. There are many ways for preparing such structures from silica-coated particles. Some of them are Langmuir-Blodgett technology, electrodeposition, spin coating, vapor deposition, and layer-by-layer (LBL) method. Silica also has the advantage of obtaining a proper hydrophobic-hydrophilic balance. This can be achieved by having the proper silylating agent on the silica shell surface. It is essential to achieve this balance so that the particles do not sink down in to the aqueous subphase but stay on the surface. If the hydrophobicity is too high, it causes the formation of surface agglomeration and disordered multilayers. The Langmuir-Blodgett technique provides the highest degree of order among methods of film preparation. Nevertheless, other techniques, particularly LBL and electrodeposition, can be used as well due to their experimental simplicity and technological importance.

Hunderi et al. [20] has worked on gold particle films where they used a vapor deposition method. However, this technique produced polydispersed and variable shaped particles and thus the films were not that good for characterization. One clear advantage of making films from solution colloids is the easiness of estimating absorption properties of both the individual particles as well as their composite film separately. Ung et al. [20] performed a detailed study on the optical properties of multi-layer films of Au @ SiO₂ particles. They used layer-by-layer method for film formation. The interparticle distance of gold particles depends on the silica shell thickness and hence is a variable parameter. The mono- and multilayers formed using LBL method are uniform and the nanoparticles are in close contact with each other. The interparticle distance can be varied from 0 to 30 nm. They conclude that as the silica thickness is increased, the plasmon peak red shifts to higher wavelength with respect to the bare gold plasmon peak. These color shifts occurs due to the dipole interaction between gold colloid particles. Maxwell-Garnet and Bruggemann come up with mathematical models that explain this phenomenon. The dipole coupling is most simply treated using Maxwell-Garnett theory [3,20] that provides an expression for the effective dielectric constant of the composite material.

3. EXPERIMENTAL SECTION

3.1. GOLD SYNTHESIS

Monodispersed gold nanoparticles are prepared by following the Turkevich method [15,21]. The minimum size of gold nanoparticles obtained using this method is around 12 to 15 nm. The following sections deal with gold synthesis experimental procedures in detail.

3.1.1. Chemical Reagents. The following chemical reagents were used for the experiments: Hydrogen tetrachloroaurate (III) $\text{HAuCl}_4 \cdot 3\text{H}_2\text{O}$ with purity of 99.99% (Au 49.5% min.), Sodium citrate (Tribasic : Dihydrate) $\text{Na}_3\text{C}_6\text{H}_5\text{O}_7 \cdot 2\text{H}_2\text{O}$ with purity of 99.9%, and Deionized water having resistivity of 18 $\text{M}\Omega\text{-cm}$. All the chemicals were used as received without any further purification.

3.1.2. Experimental Procedure. 5 ml of deionized water is first mixed with 100 μL of 13.5 mM $\text{HAuCl}_4 \cdot 3\text{H}_2\text{O}$ aqueous solution. This diluted solution is then kept on a heater / stirrer and heated until the temperature reaches 100°C while vigorous stirring. When the solution starts boiling, 225 μL of 0.3 mM $\text{Na}_3\text{C}_6\text{H}_5\text{O}_7 \cdot 2\text{H}_2\text{O}$ (dihydrate Sodium citrate) aqueous solution is added drop by drop over the period of one minute. The molar ratio of sodium citrate to hydrogen tetrachloroaurate used here is approximately 5:1. After adding sodium citrate, the color of the boiling solution changes instantly to bluish purple.

The solution is boiled (same temperature) for 8 more minutes during which transformations from initial bluish purple color to a reddish orange solution is observed. As this color is characteristic of gold sol, it marks the end of the reaction and hence the heating / stirring is stopped. The hot gold sol is then kept for cooling at room temperature

overnight before any further treatment. The concentration of gold as HAuCl_4 in the solution is $2.5 \times 10^{-4}\text{M}$ that is sufficient for further experiments.

3.2. SILANE COUPLING AGENT COATING

3.2.1. Chemical Reagents. The following chemicals were used for coating gold surface with silane coupling agents: 3-Aminopropyl trimethoxy silane $\text{C}_6\text{H}_{17}\text{NO}_3\text{Si}$ (3-APS) with purity of 97%, 3-Mercaptopropyl trimethoxy silane $\text{C}_6\text{H}_{16}\text{SO}_3\text{Si}$ (3-MPTS) and Deionized water. All the chemicals were used as received without any further purification.

3.2.2. Experimental Procedure. The gold surface is made vitreophilic either by using 3-APS or 3-MPTS. First 3-APS (or 3-MPTS) is diluted in deionized water to prepare fresh aqueous solution of silane agents at the required concentration. As gold nanoparticles of varying size have different surface areas, the concentration of 3-APS solution should be adjusted correspondingly.

Although Liz-Marzán et al. has shown that a single layer of silane coating is enough for making gold surface vitreophilic, it is seen that concentration corresponding to 5-layer coating ensures uniform single layer on the surface. The excess silane agents can then be removed by centrifuging. The concentration of silane agents used with respect to the gold size is as given below in the Table 3.1. The aqueous silane coupling agent solution is added to the gold nanoparticle solution drop wise with vigorous stirring at approximately 40°C . After 30 minutes of APS addition, the heating is stopped and the solution stirred moderately for 90 minutes. After 2 hours of continuous stirring, the solution is kept overnight without stirring before any further treatment. This ensures

complete complexation of the amine or mercapto groups with the gold surface. The surface area coverage of a single 3-APS (or 3-MPTS) molecule is approximately 4000 nm² [22].

Table 3.1. Dependence of 3-APS or 3-MPTS concentration on gold size.

Gold size (nm)	Surface area (nm ²)	Moles of silane coupling agent required per ml
2	12.6	1.83×10^{-7}
5	78.5	7.35×10^{-8}
10	314	3.67×10^{-8}
15	707	2.44×10^{-8}
20	1260	1.83×10^{-8}
40	5020	9.15×10^{-9}

3.3. ACTIVE SILICA COATING

3.3.1. Chemical Reagents. The following chemicals were used for active silica coating: Sodium silicate solution having 27% SiO₂ in 14% NaOH aqueous solution, Hydrochloric acid solution HCl of purity 36.5 to 38 w.t.% and Dowex 88 ion-exchange resin which has Na⁺ as a strong cation, this resin is in a macroporous form with 16-40 mesh size.

3.3.2. Experimental Procedure. The ion exchange resin is first washed with deionized water to remove any impurities. The washed resin is then acidified by passing

5 w.t.% of HCl aqueous solution in an ion exchange column or directly stirred in a beaker. This acidified resin is then washed with deionized water several times until the drained liquid has a pH around 6 to 7, i.e. close to neutral. This acid regenerated resin is then used as the exchange material to remove sodium cations from Sodium silicate solution having 0.54 w.t.% SiO₂. This diluted sodium silicate solution has pH around 11.3 initially which after adding the resin decreases instantaneously. The lowest pH that should be aimed while doing this mass transfer is around 10.

The APS coated gold sol is now coated with silica using active silica produced by previous treatment. The commercial sodium silicate solution consists of 27 w.t.% SiO₂. For an initial thin silica coating, the molar ratio of gold to silica i.e. ([Au] / [SiO₂]) should be around 0.1. After adding the appropriate amount of active silica to the gold sol to have the final SiO₂ concentration around 0.02 w.t.%, the solution is kept at least for 24 hours without stirring to form a thin silica layer on the vitreophilic gold surface to prevent coagulation in the Stöber method. The pH of the gold sol changes towards basicity i.e. around 8.5 to 9.0 when active silica is added.

3.4. STÖBER METHOD OF SILICA COATING

3.4.1. Chemical Reagents. The chemicals used for this step are: Tetraethylorthosilicate Si(OC₂H₅)₄ with purity 99%, Ammonium hydroxide NH₄OH having 28% NH₃ and Anhydrous Ethanol C₂H₅OH of purity 94 to 96%.

3.4.2. Experimental Procedure. After 24 hours the active silica coated gold nanoparticles are dispersed in ethanol for final silica coating using the Stöber method, which is the hydrolysis and condensation of TEOS in the presence of ammonia as a

catalyst. The ratio of ethanol to water (since gold particles are dispersed as an aqueous solution) normally used for the Stöber method is 4:1. However, higher ethanol to water ratios can be used to have different reaction conditions. Also, a ratio higher than 15:1 is not suitable for efficient silica coating. Thus, to this composite solution of ethanol and active silica coated gold sol, ammonium hydroxide and TEOS is added sequentially. TEOS concentration has to be sufficiently low to prevent excessive homogeneous nucleation. Dilute solutions of TEOS can be prepared in ethanol to keep the concentration under required limits. While adding TEOS and ammonium hydroxide, the solution is stirred vigorously followed by mild stirring for 6 hours. Then the silica coated gold particle in ethanol solution is characterized using TEM and absorption spectrometer without any further treatment.

3.5. ASSEMBLY OF SILICA COATED GOLD NANOPARTICLES

3.5.1. Chemical Reagents. Methanol CH_3OH having purity 99.8%, Poly(diallyl dimethylammonium chloride) (PDDA) medium molecular weight of purity 20 w.t.% in water, Hydrogen Peroxide H_2O_2 with purity 31.3 w.t.%, ammonium hydroxide of purity 99.99 w.t.% containing 28 w.t.% of NH_3 and microscope glass slides which are pre-cleaned and around 1 mm thick.

3.5.2. Experimental Procedure. Au @ SiO_2 composite nanoparticles are assembled using the Ung et al. procedure [18]. First, the microscope glass slides of required dimensions are cleaned by boiling in Methanol for 20 minutes. The cleaned surface is then hydroxylated by boiling in a mixture of H_2O_2 (31.3 w.t.%) and around 2-3 drops of NH_4OH (30% NH_3) for 20 minutes more. The slides are then stored in water

until further treatment. Then LBL (layer-by-layer) method is used to coat Au @ SiO₂ on this hydroxylated glass slide. The glass slide is dipped in a 1 w.t.% of PDDA aqueous solution for 30 minutes to form a PDDA layer on it. The slide is then washed with deionized water and dried using air before dipping it in the Au @ SiO₂ sol. It is kept in the sol for an hour so that silicate anions complexes with its opposite polycations from PDDA. The slide is washed again with deionized water and dried to form a monolayer of Au @ SiO₂ particles on the glass surface. For higher layers, the process is repeated i.e. the glass slide is dipped in PDDA aqueous solution and the steps as given above are followed exactly in the same order. This multi-layered Au @ SiO₂ film can then be characterized by absorption spectrometer to the check plasmon band peak position and intensity. The same procedure is also used for bare gold sol film formation.

4. RESULTS AND DISCUSSIONS

4.1. SILICA COATING OF 20 NM GOLD NANOPARTICLES

The gold nanoparticles prepared by Turkevich method using Sodium citrate as a reducing agent gives fairly monodispersed but polycrystalline particles. As shown in Figure 4.1, the size of the particles is around 18 to 20 nm. In addition, some non-spherical particles particularly triangular ones are also seen. The molar ratio of Sodium citrate to HAuCl_4 used for this experiment is around 12 but it was seen that even a ratio of 5.0 gave the same result. Thus, higher sodium citrate only increases the stability of the particles without affecting their size. These citrate-stabilized particles are then coated by either 3-Aminopropyl trimethoxy silane or 3-Mercaptopropyl trimethoxy silane to increase their affinity towards final silica coating. Though no experimental evidence was established to check the coating, it is seen that with the addition of the silane coupling agent coating that there were a larger number of silica coated particles.

The active silica coating of nanoparticles using acidified sodium silicate solution is done after the 3-APS coating. However, various attempts were made to have an appreciable thickness of silica using this method; the silica thickness was unnoticeable under TEM. Nevertheless, when some ammonia was added as a catalyst under constant stirring, the silica coating could be seen after 6 hours on some particles as shown in Figure 4.2. The gold used for this particular experiment was not made by Turkevich method but was bought from a commercial manufacturer Ted Pella INC, CA. The size of this gold sol is also around 20 nm but the reducing agent is unknown as the process is a commercial secret. These gold sols have same characteristics as that made by Turkevich

method hence gives the same result for similar conditions. Hence, it is understood that the active silica condenses on gold surface if ammonia is added with ethanol as a solvent.

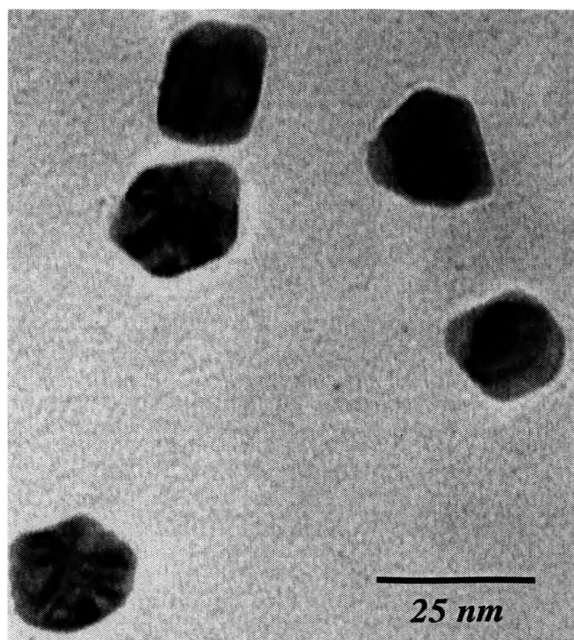


Figure 4.1. Bare 20 nm Au nanoparticles prepared by Turkevich Method.

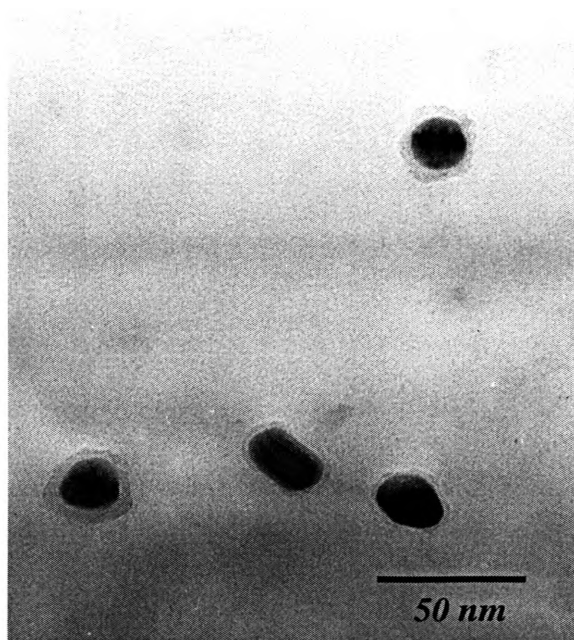


Figure 4.2. Active silica coating on 20 nm Au nanoparticle.

Nevertheless, as said above not all particles were coated by active silica. Some of the other variations undertaken to have an appreciable silica coating on gold surface were high temperature, higher silica concentration with respect to gold and higher condensation time but met with no success. The typical result that is seen when active silica is added is a huge silica matrix on which gold particles are embedded. This silica matrix formed does not have any particular shape and mostly condensed lightly. However, both 3-APS and active silica addition does increases the final condensation of silica on gold. This is seen in Figure 4.3 that shows 5 nm silica coating on 20 nm gold

particles after TEOS hydrolysis and condensation by using the Stöber method. The gold surface is treated with 3-APS and active silica and is kept for at least 24 hours before undergoing the Stöber method. The silica coating is uniform around the surface with monodispersed size. Homogenous nucleation for this condition is also very minute due to low TEOS concentration. The concentrations used for this experiment are TEOS is 47.9 μM , NH_3 is 0.2117 M, and, H_2O is 7.873 M while the volumetric ratio of ethanol to water is 6.0. Figure 4.4 shows the experimental condition for thicker silica coating around 10 nm for which the only difference is the amount of silica added.

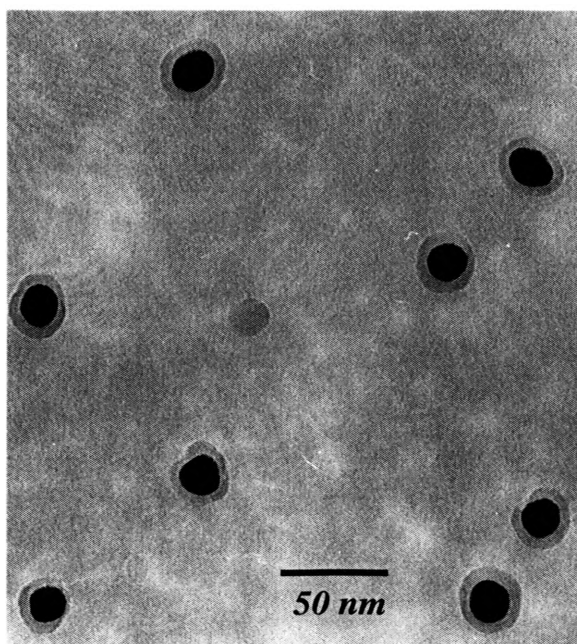


Figure 4.3. 5 nm silica coating on 20 nm Au nanoparticles.

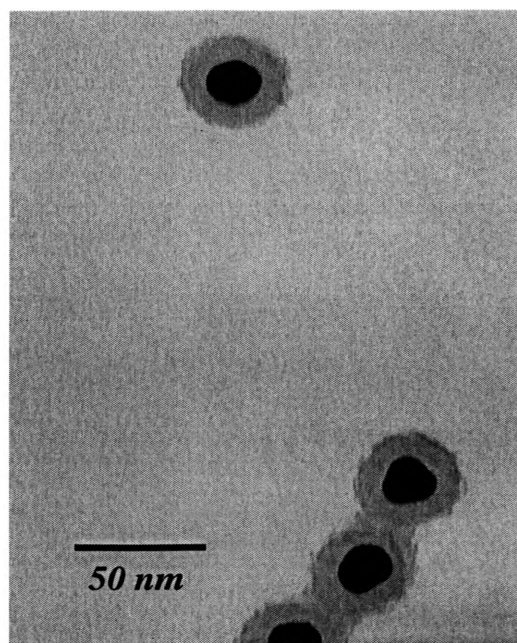


Figure 4.4. 10 nm silica coating on 20 nm Au nanoparticles.

The silica surface is noticeably rough which sometimes happens due to high ammonia concentration. The homogenous nucleation is also higher than previous conditions as higher TEOS is added. Necking or joining of coated particles is detected

with higher TEOS addition. This necking is due to various reasons some of which are hydrogen bonding, siloxane bond formation between two hydrolyzed silica molecules, Vander Walls force, drying on grid or sometimes even gelling i.e. silica is not fully condensed and gels if the pH is close to neutral. However, at this condition all the particles are coated with constant silica thickness. The TEOS concentration used for this condition is 192 μM keeping all other components constant. The next logical condition of thicker silica shell was tried by increasing TEOS concentration keeping the other values constant. The silica size increased to 20 nm when the TEOS concentration is increased to 479 μM . Homogenous nucleation also increased for this experiment as did the presence of necking. This is as shown in Figure 4.5. While for much higher TEOS concentration of 958 μM , thicker silica coating of 30 nm is seen. The TEM for this experiment is shown in Figure 4.6 and have higher necking and gold free silica than all previous conditions.

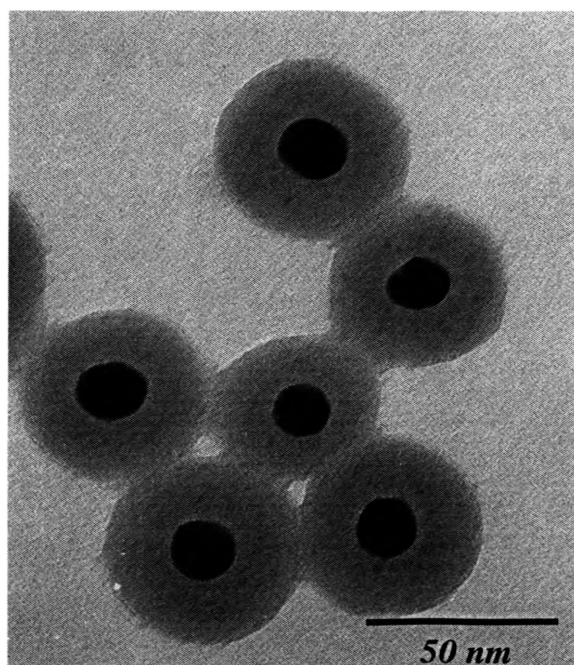


Figure 4.5. 20 nm silica coating on 20 nm Au nanoparticles.

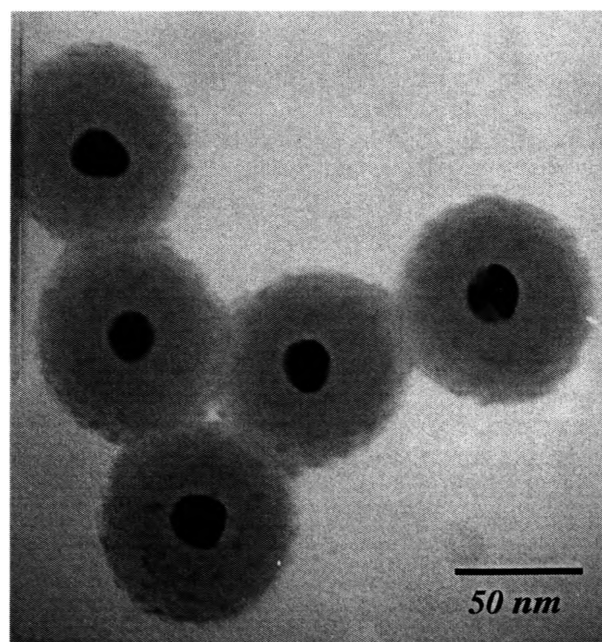


Figure 4.6. 30 nm silica coating on 20 nm Au nanoparticles.

Although all the previous experiments were done by single TEOS addition, the results achieved were same when TEOS was added in batches. Figure 4.7 shows the final silica coating after 12 hours when TEOS was added in two batches to have a concentration from 47.9 μM to 251 μM . The expected silica thickness was higher than 10 nm but the actual thickness achieved was around 12 nm. In addition, homogenous nucleation was evident with some necking as expected. It is seen that batchwise addition does not affect the necking or homogenous nucleation in any way. Further batchwise addition experiments were done on 20 nm gold nanoparticle by adding TEOS in six batches from initial concentration of 48.2 μM to final concentration of 1.01 mM over the period of 1 day. However, the expected silica thickness of 80 to 100 nm after 1 day was not achieved. The resulting particles are shown in Figure 4.8 which shows that the thickness is around 15 nm with very high homogenous nucleation and necking.

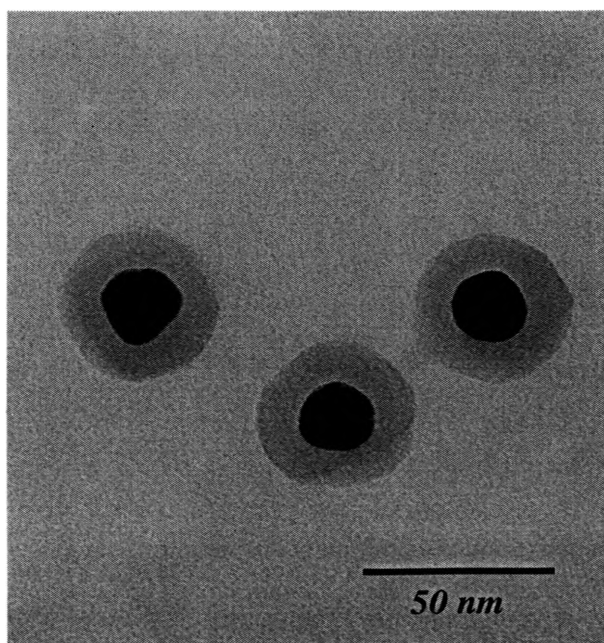


Figure 4.7. 10 nm silica coating on 20 nm Au nanoparticles by batchwise TEOS addition.

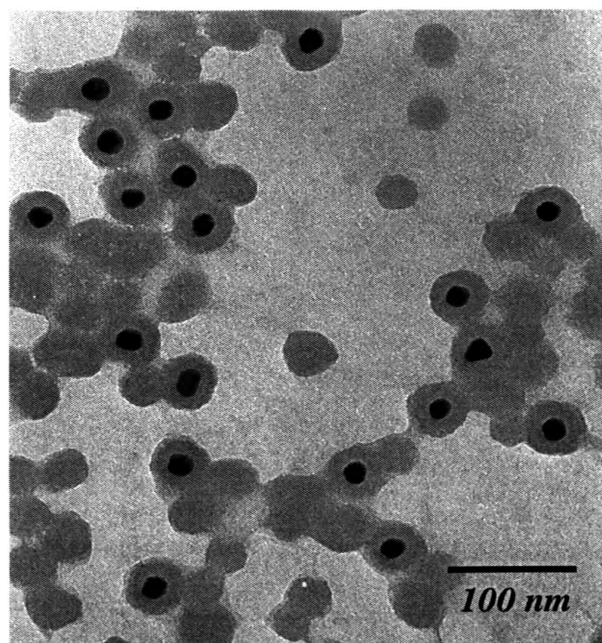


Figure 4.8. Batchwise silica coating on 20 nm Au for an expected thickness of 80 to 100 nm.

It can be seen that the gold free particles have the same size as silica coated gold particle. This can happen due to extended nucleation period that results because of numerous batchwise TEOS addition. As TEOS hydrolysis and condensation is a two-step process of nucleation and growth, after every addition, the nucleation sets in and creates higher probabilities for silica to condense on the already nucleated particles. This increases homogenous nucleation to much greater extent. In addition, after gold is coated appreciably by silica, the rate of silica addition decreases as compared to that for smaller gold free particles formed at the initial stage. The ethanol to water ratio has a major effect on the silica condensation on gold particles. Figure 4.9 shows the silica coating produced when the ratio is kept higher than 2.0. The coating is uniform and monodisperse as usual with thickness around 10 nm. However, when this ratio is reduced below 2.0 (i.e. Figure 4.10), no coating on the gold surface is seen for the same TEOS and ammonia values.

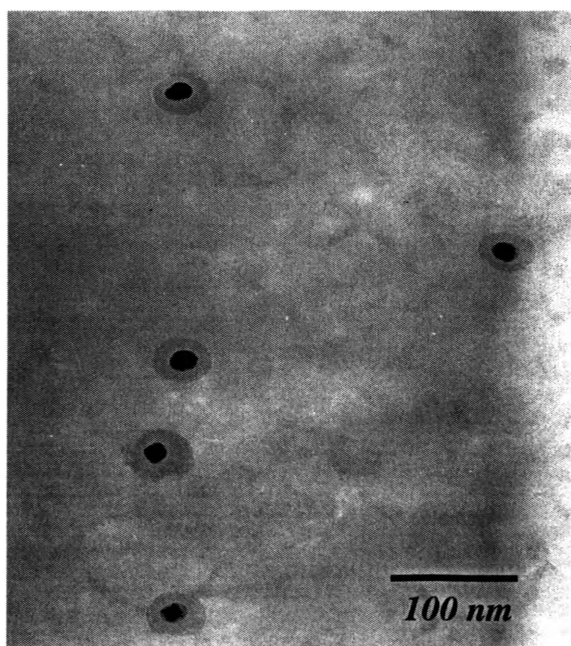


Figure 4.9. 10 nm silica coating on 20 nm Au nanoparticles for EtOH/H₂O ratio higher than 2.0.

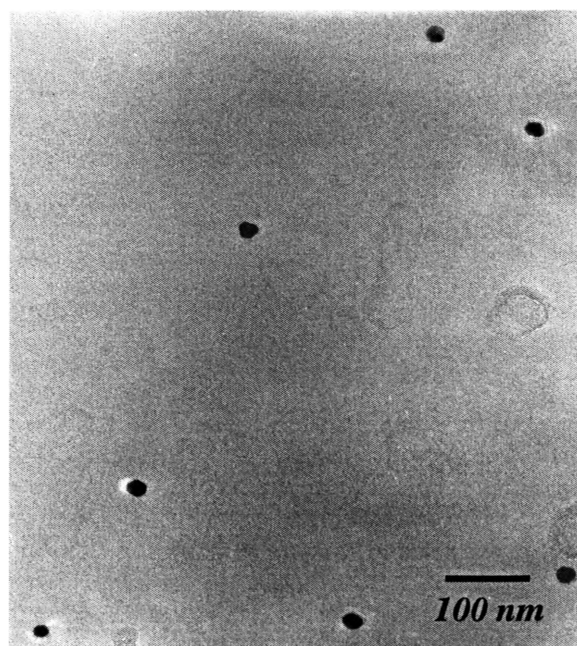


Figure 4.10. No silica coating on 20 nm Au for EtOH/H₂O ratio less than 2.0.

This can be explained from the fact that silica has lesser solubility in ethanol as compared to that in water. The higher water content prevents silica condensation since it prefers to remain as soluble silica in the aqueous solution. Thus, the gold surface remains uncoated if the EtOH/water ratio goes below some certain limit. Figure 4.11 shows a non-typical result for the silica coating that consists of no pre-coating of the gold surface with 3-APS and active silica. In this experiment, the gold surface was directly coated with silica using the Stöber method. Due to low polarity of ethanol as compared to water, gold aggregates were formed in the solution but most of them remain un-aggregated. Silica coated on the gold surface quite uniformly but was not monodispersed. This non-uniformity is due to vitreophobic surface of gold. Silica condenses on the surface in a non-linear way and hence prevents constant size.

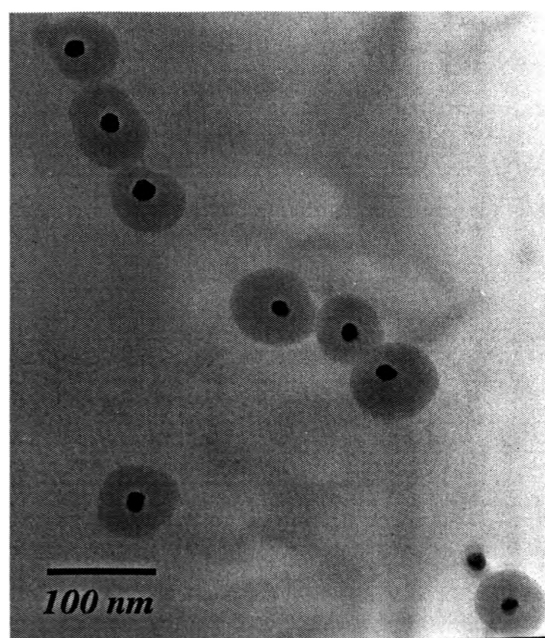


Figure 4.11. Silica coating on 20 nm Au nanoparticles without any pre-coating with 3-APS and/or active silica.

Though all the above experiments are done on 20 nm particles, it is seen that when the conditions for 20 nm are applied to 15 nm particles, the results are almost same. This can be explained by studying the following facts in the table below. Table 4.1 shows that the surface area of 20 nm particles is 43% higher than that of 15 nm particles. In addition, the number of particles per ml for 15 nm is higher than that of 20 nm by 58%. Hence, it is expected that the results for 20 and 15 nm should be approximately same for similar conditions. When 20 nm is compared similarly with 10 nm particle, a huge difference both in the surface area and in number of particles per volume is seen. The surface area of 20 nm is 75% higher and number of particles of 10 nm 87% higher than 20 nm. Hence, the following conditions that are done for 15 nm particles can be compared to 20 nm ones directly. 3-APS coupling agent has a remarkable effect on the effectiveness of silica coating on gold surface. Its coating increases the uniformity of silica around gold and thus the final monodispersity.

Table 4.1. Characteristics of different sized Au particles.

Gold size (nm)	Surface area (nm ²)	Number of particles per ml at 0.03 Au w.t.%
2	12.6	7.04×10^{13}
5	78.5	4.50×10^{13}
10	314	5.63×10^{12}
15	707	1.67×10^{12}
20	1260	7.04×10^{11}
40	5020	8.80×10^{10}

However, there was no major dependence of number of 3-APS layers on final silica coating. Figure 4.12 shows the result for silica coating for five 3-APS layers on gold surface as compared to ten 3-APS layers (Figure 4.13). The only difference seen is slightly thicker coating and high homogenous nucleation for increased 3-APS layers. Increased homogenous nucleation is the result of increased nucleation sites for high 3-APS concentration. Each molecule has the capacity to form gold free silica due to its siloxane bond formation tendency. Also higher silane layers on gold increases its affinity towards silica deposition and hence increases the silica thickness.

It should be noted that all the previous experiments were done with direct addition of TEOS. However, when TEOS was added in a continuous manner keeping other additions batchwise, the results were surprisingly unchanged. Figure 4.14 is one such experiment where TEOS is added at a rate of 0.04 ml/hr for 1 hour (TEOS is diluted in ethanol) for total concentration of 122 μM . The figure shows perfect coating on gold surface with almost no homogenous nucleation and thickness of 10 nm. The effect of higher temperature on the silica coating of 20 nm gold was also undertaken with unexpected results. As discussed before silica hydrolysis and condensation kinetics are directly proportional to temperature. When silica is coated at a higher temperature such as 50°C, the gold nanoparticles are aggregated due to high collision rate and silica forms non-spherical condensed matrix around gold. However, when heating was applied after 2 hours of stirring at room temperature, the particles were coated by a very thin silica layer of 3 nm. Some silica mass around the gold particles can also be seen. Thus, heating does not help silica coating on gold surface and the thin layer is the result of the initial stirring at room temperature. This is as shown in Figure 4.15.

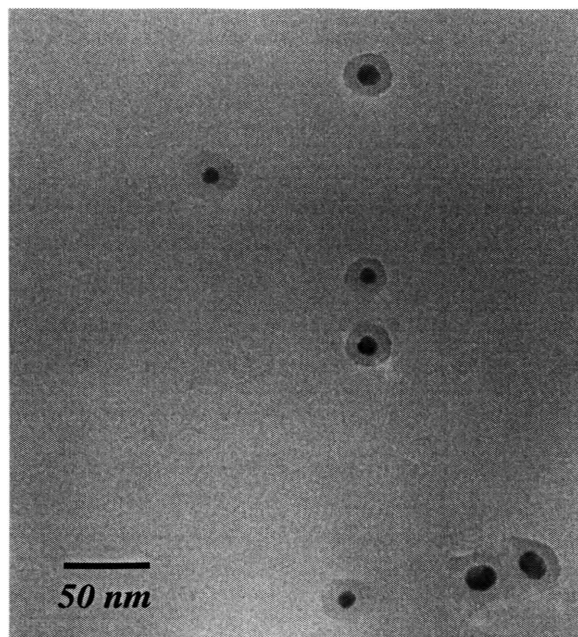


Figure 4.12. Coating on 15 nm Au nanoparticle after five APS layers of pre-coating.

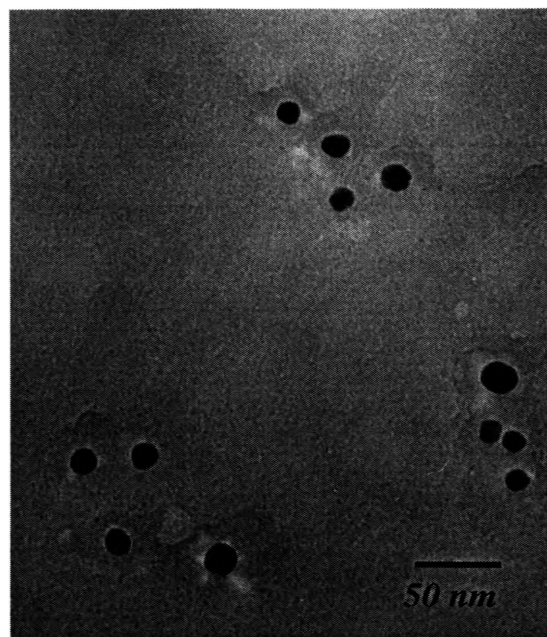


Figure 4.13. Coating on 15 nm Au after ten APS layers of pre-coating.

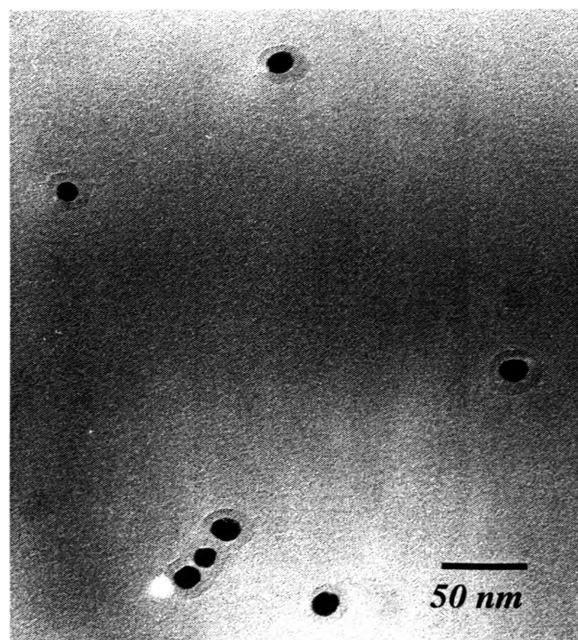


Figure 4.14. Silica coating on 15 nm Au when TEOS is added in a semibatch way.

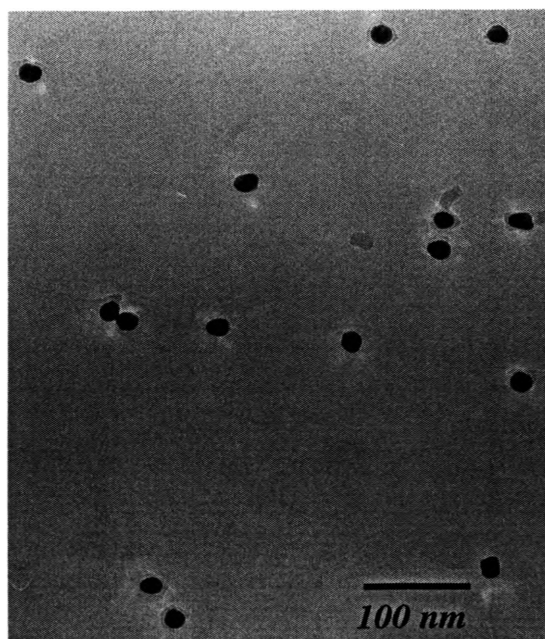


Figure 4.15. Heating effect on the silica coating of 20 nm Au particle.

While different TEOS concentrations results in various silica thicknesses, the effect of different ammonia on silica coating was also studied. Figure 4.16 is the micrograph for silica coating at lower ammonia content whereas Figure 4.17 is that for double the concentration of ammonia. There is almost no difference between the particles formed at the two conditions except that for lower ammonia concentration, silica was less spherically defined. This explains the role of ammonia as a morphological catalyst in the Stöber method.

Active silica preparation procedure affects the final silica coating in the Stöber method. One of the methods is directly contacting acid like HCl or H₂SO₄ aqueous solution with the sodium silicate solution with continuous rapid stirring. The major disadvantage with this method is that while adding the acid solution, some very low pH pockets are created.

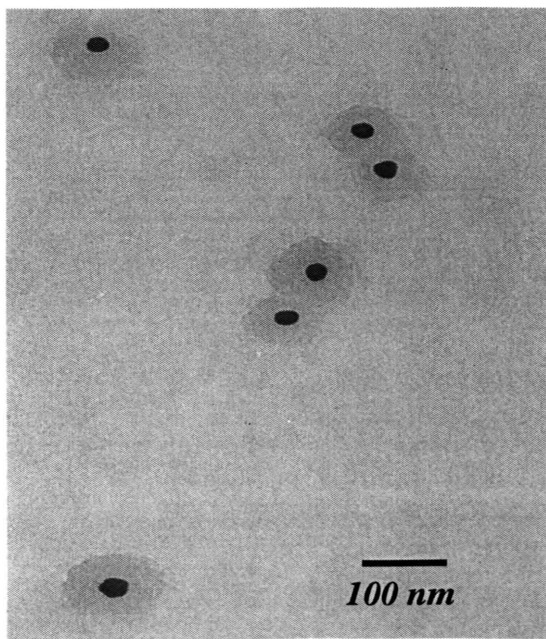


Figure 4.16. Silica coating on 20 nm Au for lower ammonia concentration.

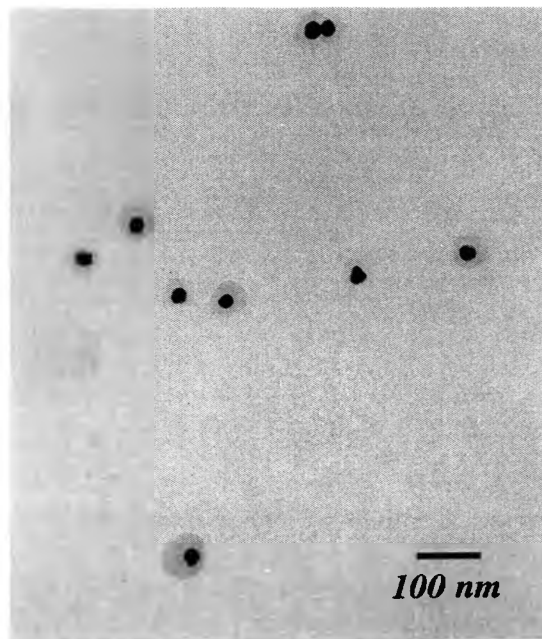


Figure 4.17. Silica coating on 20 nm Au for higher ammonia concentration.

Silica gel forms in these pockets which when added to APS coated gold colloidal sol attaches to the nanoparticles. This prevents any silica coating on gold surface by the Stöber method and forms red precipitated gold aggregates after some time in ethanol. The TEM for this method of active silica preparation is shown in Figure 4.18.

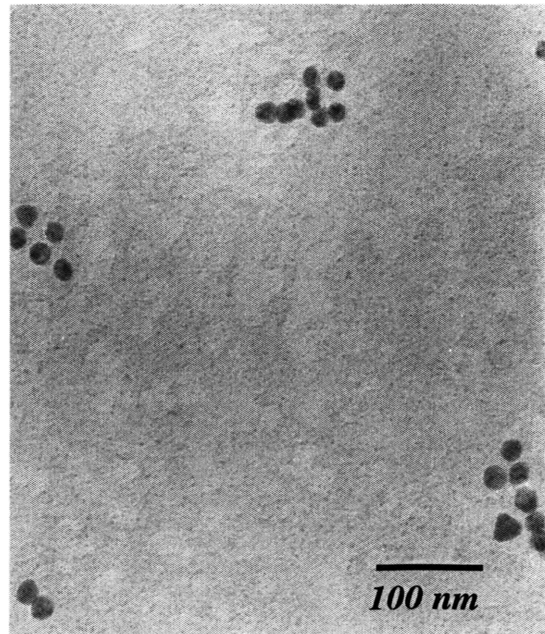


Figure 4.18. Gelling due to direct contact of acid with sodium silicate while preparing active silica.

4.2. SILICA COATING ON 10 NM GOLD NANOPARTICLES

Ten nm gold nanoparticles were coated by the same procedure used that for 20 and 15 nm particles. Figure 4.19 shows the particles formed after silica coating on 10 nm gold for TEOS concentration of 123 μM and NH_3 concentration 0.174 M, H_2O concentration 6.49 M and EtOH/ H_2O ratio of 7.5. It also shows that silica is polydispersed and not very spherical either. Necking that was minimal for 20 and 15 nm particles is now too high to preserve the spherical shape and thus looks coagulated.

Although most of the gold particles were spherical after coating, large percentage of particles were still in silica mass and not spherically shaped. Thus, necking is quite high when coating gold particles smaller than 15 nm. As indicated earlier necking can be due to various reasons viz. hydrogen bonding, drying effects on grid or siloxane bond formation between condensed silica molecules. Figure 4.20 is a variation of the above experiment where EtOH/H₂O ratio is increased to 12.0 with decreased concentration of H₂O to 4.23 M. This setup gives much better result than the lower EtOH/H₂O ratio but coagulation and necking is still present although reduced.

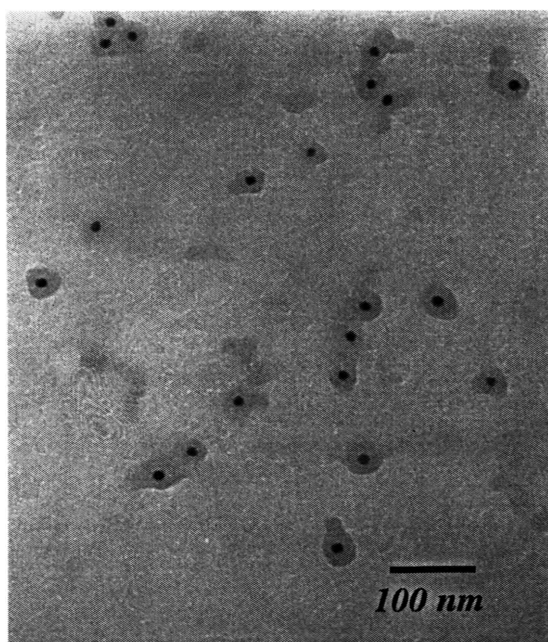


Figure 4.19. Silica coating on 10 nm Au for EtOH/H₂O ratio of 7.5.

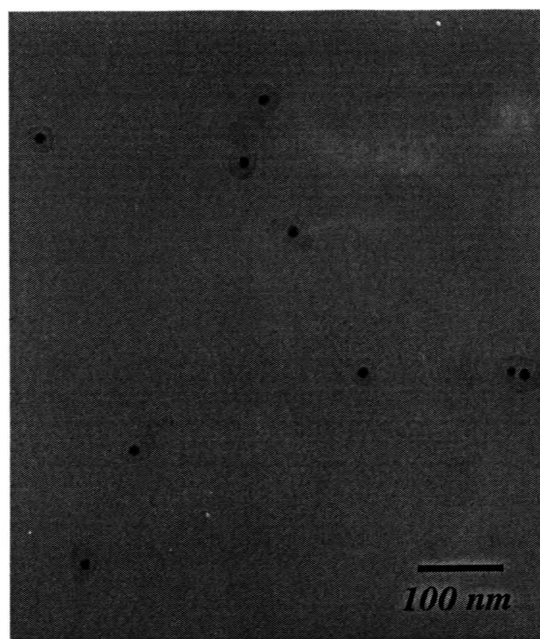


Figure 4.20. Silica coating on 10 nm Au for EtOH/H₂O ratio of 12.

4.3. SILICA COATING ON 5 NM GOLD NANOPARTICLES

Smaller gold nanoparticles such as 5 and 10 nm have the same problem of extensive coagulation and necking. The results for 5 nm gold particles were no better

than 10 nm ones due to coagulation and necking and hence, there are very few single silica coated gold as compared to 10 nm particles. Figure 4.21 shows the silica coated particles formed when TEOS concentration is 192 μM , and concentrations of NH_3 and H_2O are 0.212 M and 7.87 M respectively with EtOH/ H_2O ratio of 6.0. As expected, the coagulation is still present with almost no single silica coated particles. The micrograph shows that silica is coated on gold surface but then coagulates in a chain like manner. This coagulation is mostly due to insufficient surface charge on silica. This surface charge can be increased by forming thicker silica shells or by adding higher ammonia. When higher TEOS and/or ammonia concentrations are used for more perfect spherical coating, the result remains same. Figure 4.22 shows the silica coating on 5 nm particles at higher TEOS concentration i.e. 3.06 mM while keeping other components same. It shows more perfectly spherical silica on gold but due to high TEOS, the homogenous nucleation is also high.

Figure 4.23 shows silica coating formed at conditions where TEOS concentration is 756 μM and NH_3 is 0.417 M. For this condition, the silica surface is rougher (due to high ammonia content) with lots of silicates in the background as gold free silica particles. However, for both these variations, the coagulation and necking still existed. Hence, they are not the perfect conditions for coating 5 nm gold particles. Coagulation can be decreased if the particles are diluted after coating silica on them. However, this can be proved only after assuming that coagulation does not occur in situ but while drying the solution on the grid. Thus, after silica coating excess ethanol (3 times of original solution) was added. After proper homogenization, the grid is taken. Figure 4.24 shows the results for silica coating at this condition.

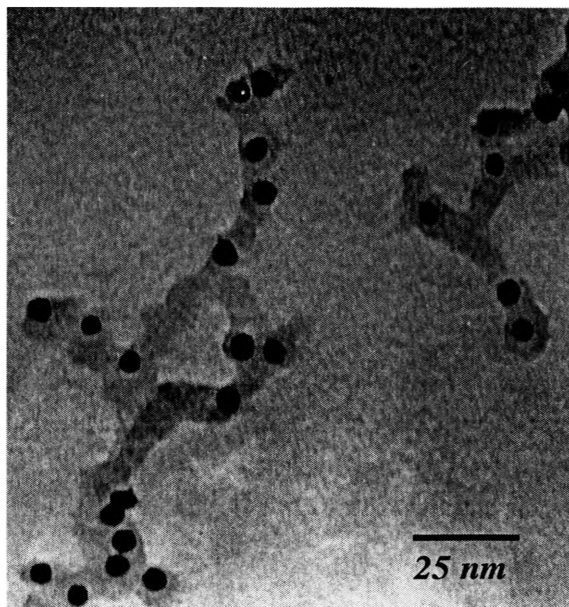


Figure 4.21. Silica coating on 5 nm Au for TEOS=192 μ M and NH_3 =0.212 M.



Figure 4.22. Silica coating on 5 nm Au for TEOS=3.06 mM and NH_3 =0.212 M.

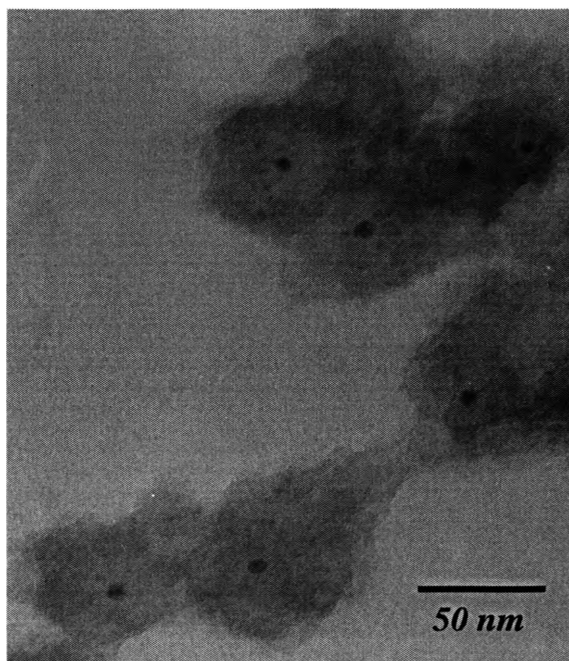


Figure 4.23. Silica coating on 5 nm Au for TEOS=756 μ M and NH_3 =0.417 M.

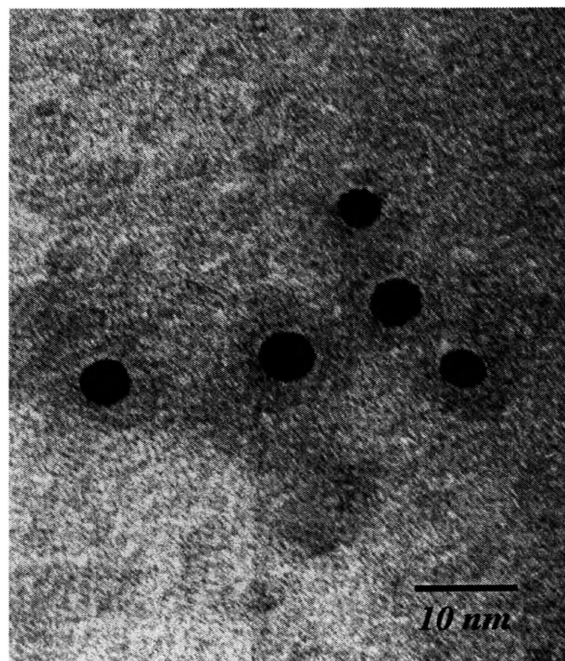


Figure 4.24. Effect of ethanol dilution on coagulation of silica coated 5 nm particles.

Although the silica coagulation and necking was reduced, fewer particles are seen due to final the dilution. Final dilution does give better results, i.e. larger single silica coated particles are seen than non-dilution process. Figure 4.25 shows the result for higher final dilution (10 times the original solution) after TEOS coating on gold. The spherical shape of silica is maintained to form some single silica coated gold nanoparticles. However, gelling is persistent with homogenous nucleation. Hence, dilution seems only to prevent coagulation to some extent but the collisions between coated particles are still high enough to have maximum single particles. Also, with higher dilution, the particles could not be seen through microscope and hence cannot be analyzed.

One of the causes of coagulated silica after TEOS condensation could be the active silica added initially. As this active silica is not detected on the gold or not condensed completely, it can remain in the solution as soluble silica. Thus, after addition of ethanol the solubility decreases to form insoluble silica that could transform into its coagulated form. This explanation is checked by adding ethanol after active silica to make it insoluble and thus increase the probability of gold precoating. This could possibly reduce the final coagulation after TEOS addition. Figure 4.26 shows the silica coating produced using the method as discussed above. It shows that the coagulation is still present and silica is spherically coated on gold. Thus, active silica is not the reason causing final silica gelling.

One of the possible explanations for coagulation is also the drying effect on the TEM grid. In one of the experiments, the grid was taken by adding drops of the final solution to a heated grid. This grid was heated to a temperature to let the ethanol in the

solution evaporate as soon as possible and thus leave only silica coated particles on it. When ethanol evaporates rapidly due to heat, it should give very less time for silica to coagulate with other silica particles and hence remain single and spherical. Figure 4.27 shows that the result is same and coagulation is still present. Again, the spherical shape of silica can be seen after coating the gold surface. Thus, heating seems only to repeat the previous results and does not help to form higher percentage of single coated particles on the grid.

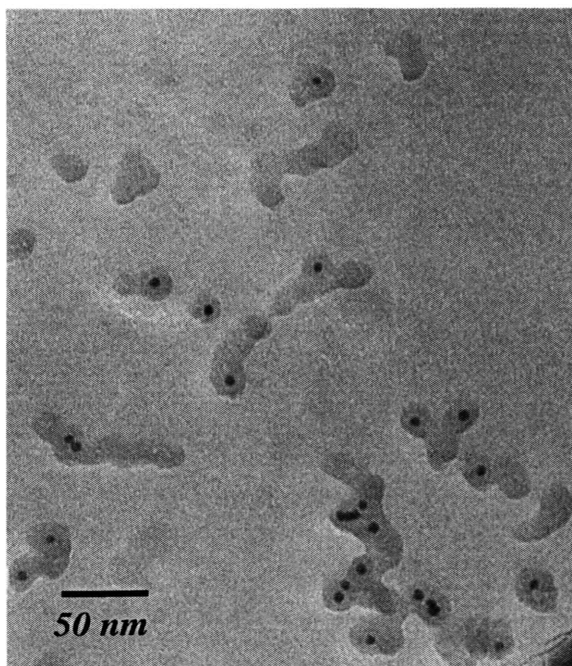


Figure 4.25. Effect of higher dilution on coagulation of silica coated 5 nm gold nanoparticles.

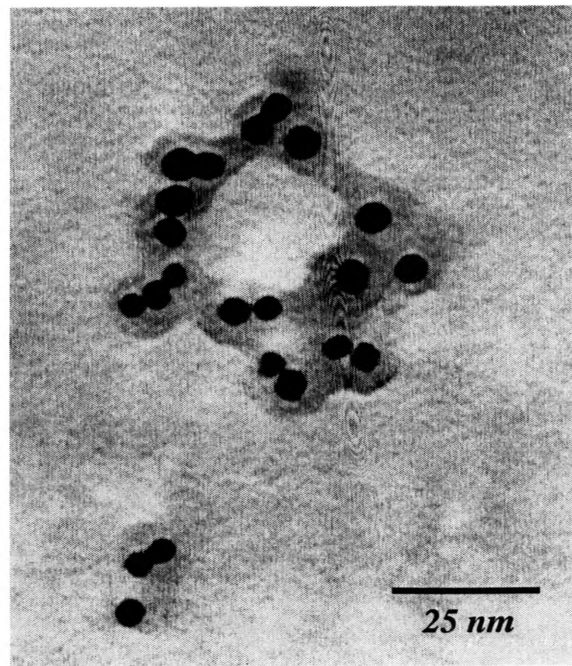


Figure 4.26. Initial addition of ethanol for complete condensation of active silica.

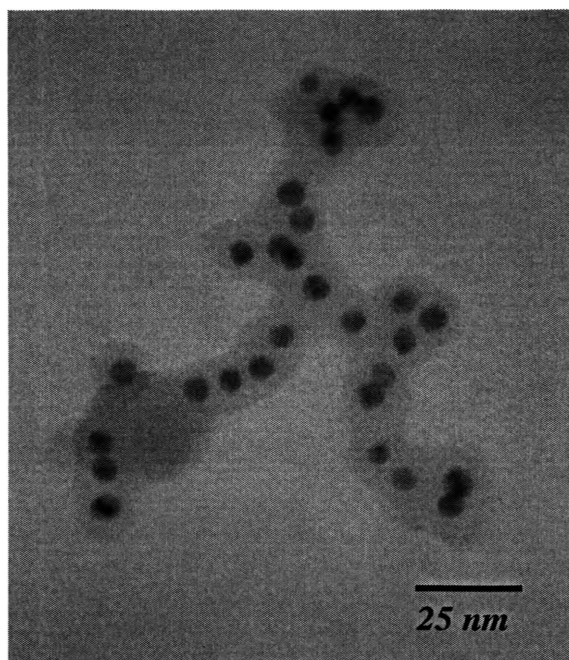


Figure 4.27. Effect of grid heating to prevent coagulation of silica while drying the grid.

4.4. SILICA COATING ON 40 NM GOLD NANOPARTICLE

Although 40 nm particles are easy to coat as 20 and 15 nm, some different coating kinetics can be seen for such larger particles. Figure 4.28 shows the silica coating performed on 40 nm gold particle. The striking feature in this micrograph is the thin silica coating on gold with lots of gold free silica around it. The silica thickness is around 10 nm and is monodispersed in size. The excess homogenous nucleation can be due to the slower deposition rate on the gold surface as compared to the rate of silica condensation. This effect creates higher nucleation sites that favor gold free silica condensation. As higher TEOS is used up for homogenous nucleation, the silica thickness on gold is very thin though monodispersed. The silica thickness can be increased by adding higher TEOS but, that will also increase the homogenous nucleation.

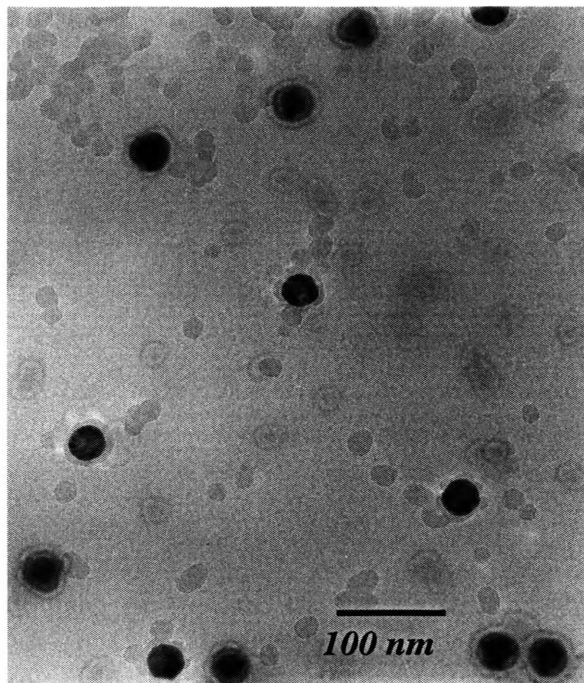


Figure 4.28. Silica coating on 40 nm Au nanoparticle.

4.5. OPTICAL RESULTS OF 20 NM GOLD NANOPARTICLES

The silica coated gold particles are characterized by absorption experiments to check their optical properties. This experiment was done using an absorption spectrometer. The absorbance of the solution is calculated from the spectrometer as per the Beer's law. This law states that the absorbance of the material is directly proportional to the concentration of the light sensitive material in the mixture. The mathematical version of Beer's law is:

$$A_{\lambda} = -\log_{10} \left(\frac{S_{\lambda} - D_{\lambda}}{R_{\lambda} - D_{\lambda}} \right) \quad (5)$$

where S is the sample intensity at wavelength λ , D is the dark intensity at wavelength λ , R is the reference intensity at wavelength λ .

The absorption spectrum for bare gold particles solution shows the plasmon peak around 525 nm. This peak position is characteristic of gold. Figure 4.29 shows the results for layer-by-layer self assembly of bare gold particles for three layers of films. The solution spectrum is also shown besides the film spectra. It shows that the peak position for the film spectra are largely red shifted as compared to the solution spectrum. The peak is around 600 nm and is due to the aggregation that occurs due to the absence of any protective layer on gold against aggregation. Figure 4.30 shows the solution and film spectra for gold coated by 3-APS on it. Here too the solution peak is around 525 nm but the film spectra (again three layers) have a peak around 600 nm due to aggregation. Thus, the 3-APS molecular layer is also not enough to prevent gold aggregation.

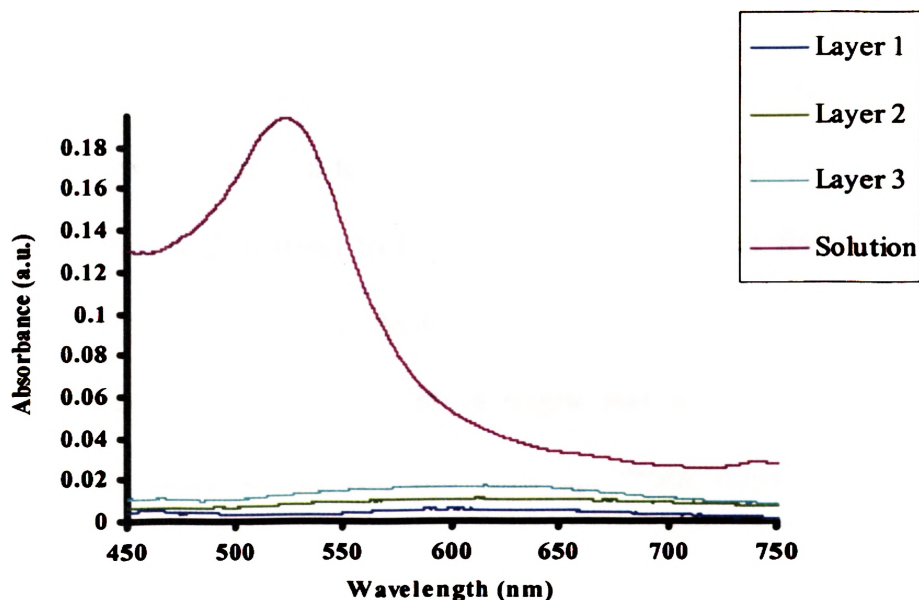


Figure 4.29. Optical spectra of Bare Au. (both films and the solution spectra)

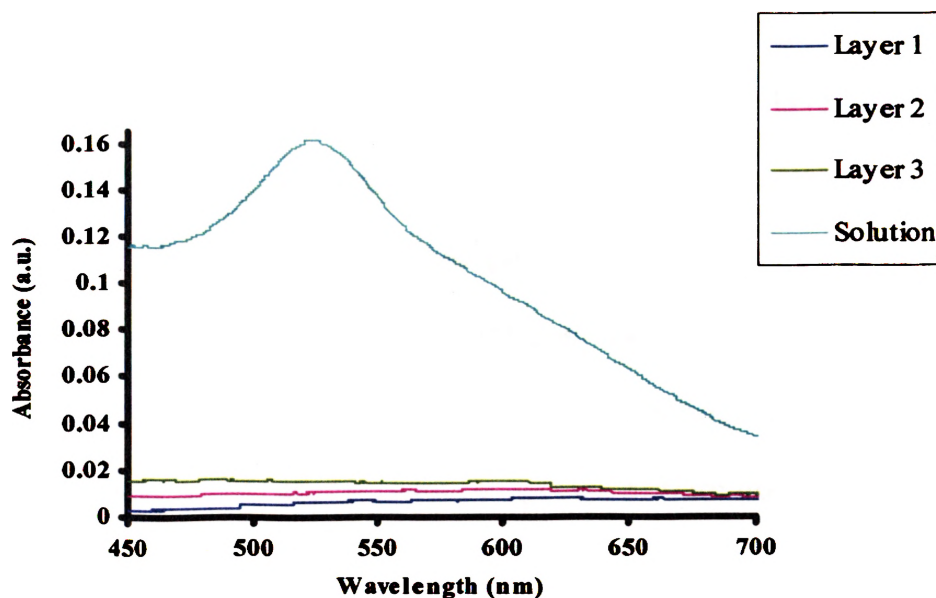


Figure 4.30. Optical spectra of Au coated by 3-APS. (both films and the solution spectra)

However, when silica is coated on gold the film spectra shows some stability. Figure 4.31 shows the spectra for 20 nm gold coated by 5 nm silica. The solution plasmon peak is now red shifted to higher wavelength. This peak is around 530 nm or a shift of around 5 nm with respect to bare gold spectrum. The film spectra for 10 layers are also plotted in the same figure. As the number of layers is increased, the absorbance increases as expected but there is also a slight red shift towards the solution peak position. But even after 10 layers, the film spectrum does not touch the solution absorbance value. The tenth layer peak position is around 520 nm which is still 10 nm less than the solution plasmon peak.

Figure 4.32 also shows optical spectra for silica coated on gold for 10 nm silica coating. The film spectra show the same trend as for 5 nm silica coated gold. The red shift occurs as the number of layers is increased but never reaches the solution

absorbance. For thicker silica coating of 20 nm, the result is same as shown in Figure 4.33. The only difference is that the peak position of tenth film layer for 20 nm silica coating is closer to the solution spectral peak position. When this coating is increased to 30 nm, this trend continues and thus the peak position for the last layer is closer to the solution spectra than corresponding 20 nm coating as shown in Figure 4.34. Other than that the optical spectra follows the same trend as all previous silica coated particles. Figure 4.35 is the comparison of all the solution spectra of bare gold and the ones coated by 3-APS and silica. To avoid the effect of concentration on the absorbance values, the spectra are normalized with respect to the peak value of each spectrum. The plasmon peak position for bare gold is around 525 nm as said earlier that does not change when 3-APS is coated on it.

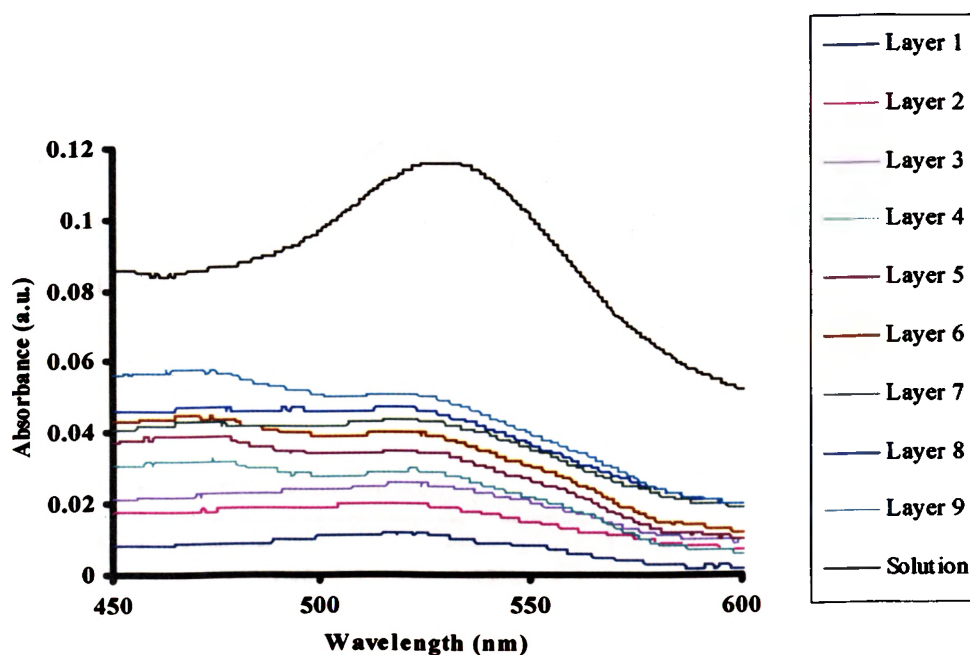


Figure 4.31. Optical spectra of Au coated by 5 nm silica. (both films and solution spectra)

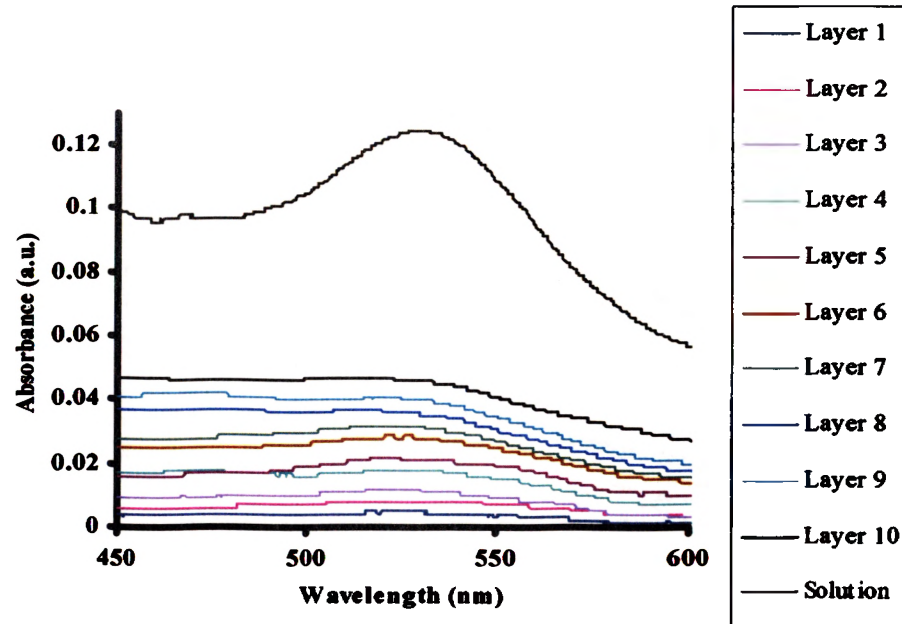


Figure 4.32. Optical spectra of Au coated by 10 nm silica. (both films and solution spectra)

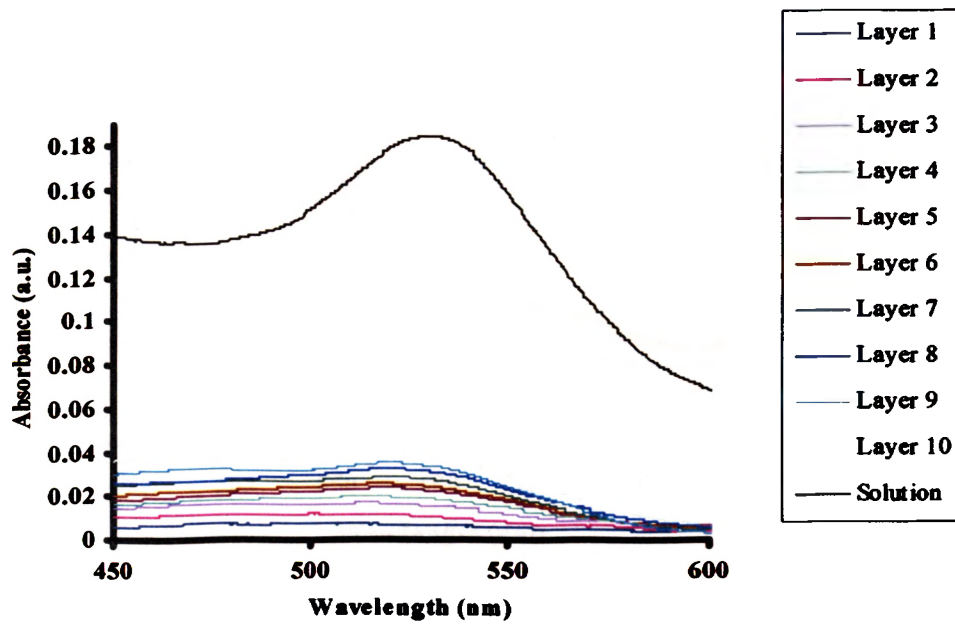


Figure 4.33. Optical spectra of Au coated by 20 nm silica. (both films and solution spectra)

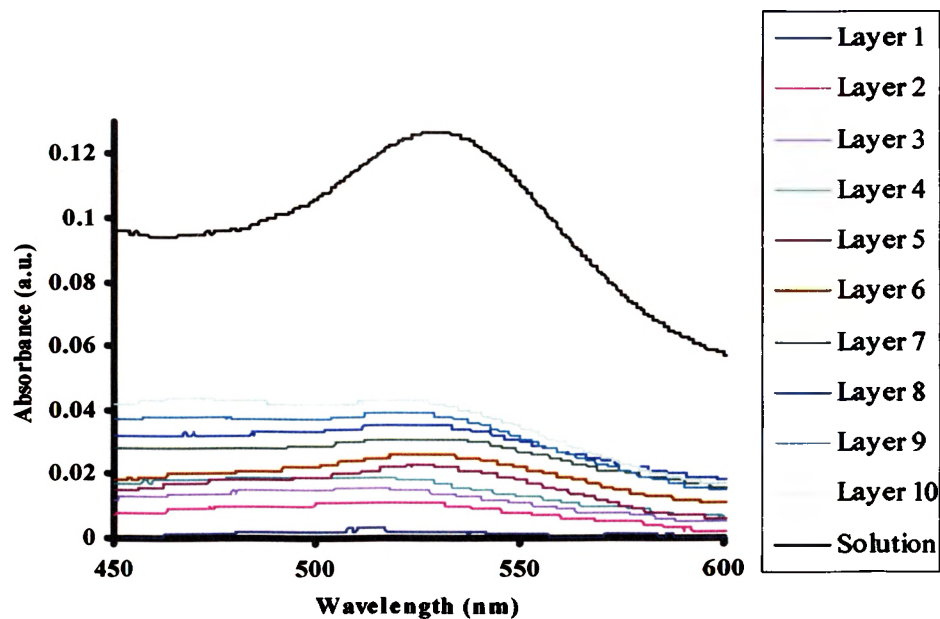


Figure 4.34. Optical spectra of Au coated by 30 nm silica. (both films and solution spectra)

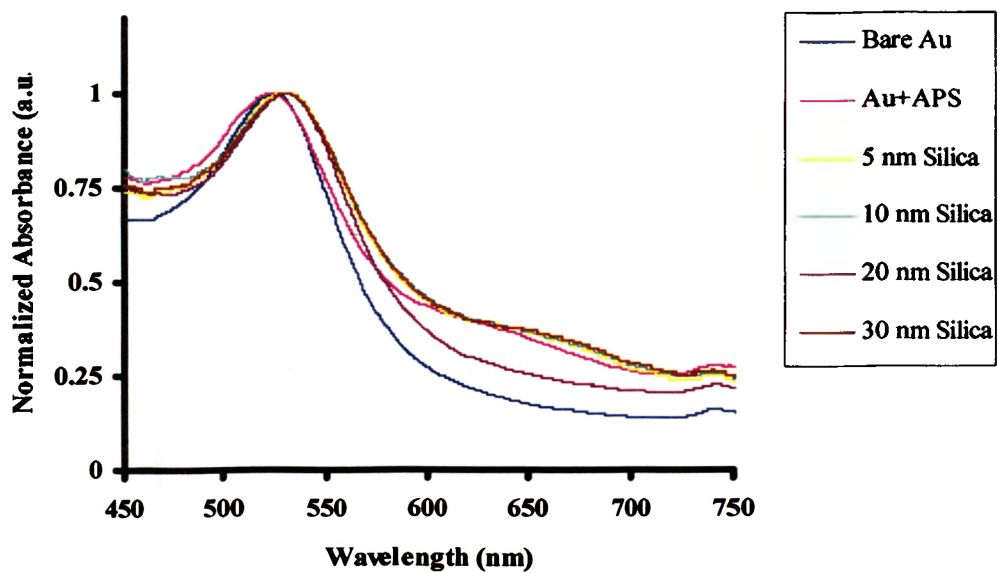


Figure 4.35. Normalized solution absorbance spectra of 20 nm Au compared with 3-APS and various thickness of silica.

The peak position for 3-APS coated gold is also around 525 nm that proves the fact that coating is in molecular level and hence not noticeable. However, as silica is coated on the gold surface the red shift is noticeable and the peak position red shifts to higher wavelength to around 530 nm. This shift of 5 nm is due to the fact that the refractive index of silica shell is higher than that of the solvent ethanol which is used in the Stöber method [18]. Thus, if the refractive index of shell layer is same as solvent, it has no effect on the plasmon band and the shell is invisible. Although for thicker silica coating the red shift should be higher, no larger shifts for 10, 20 and 30 nm silica coating is seen. In fact, all silica coating above 5 nm lie around 532 nm a slight shift of 2 nm with respect to 5 nm silica coating. This trend is because with thicker shells, there is little change in the interactions between the dipole and the optical light. This makes gold less sensitive to thicker silica coating. Figure 4.36 shows the same result but in another format.

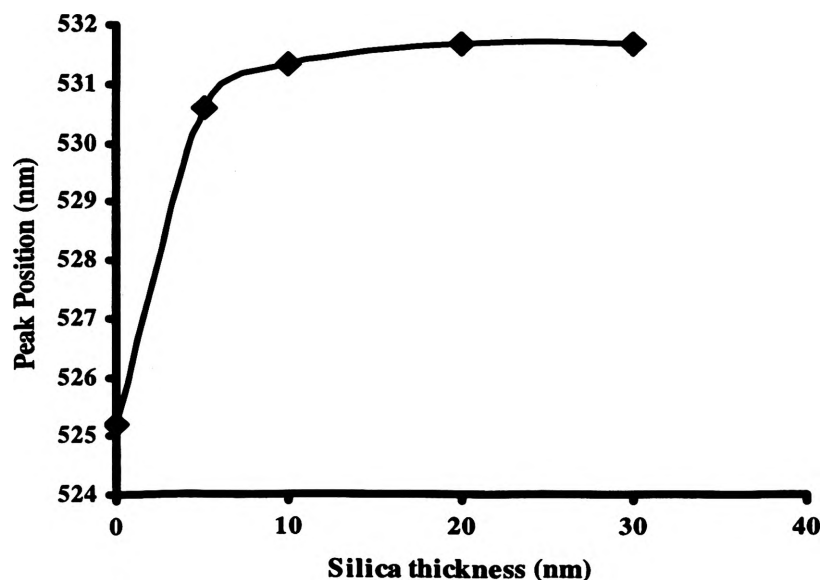


Figure 4.36. Variation of peak position with different thicknesses of silica.

5. CONCLUSIONS

Gold nanoparticles prepared by the Turkevich method are monodispersed and can be coated by silica using the Stöber Method. But, this method works well only for 20 and 15 nm gold particles and not for 10 and 5 nm particles. In addition the silica thickness achieved was up to 30 nm thick with some homogenous nucleation. However, for coating thicker than 30 nm, the homogenous nucleation was extremely high due to elongated nucleation period and hence not a suitable condition.

3-APS coating does make gold vitreophilic and hence increases the chances of silica coating on gold. Active silica is also not coated on gold but it definitely increases the TEOS condensation and hence better silica coating. Hence, active silica should be added to the gold sol but with proper control of conditions to prevent excessive homogenous nucleation. Also, some of the typical conclusions found in the Stöber method coating were as follows.

The ethanol to water ratio is important for silica condensation. For higher water content in the solution, the silica doesn't precipitate and hence remains as soluble silica without any coating on gold. The silica addition process doesn't affect its coating kinetics. Hence, the results for both direct and continuous additions of TEOS are the same. In addition, ammonia does act like a morphological catalyst and ensures spherical shape of silica while coating. But, with higher ammonia addition, the silica surface becomes rough probably due to the active silica present in the solution.

The main problem with smaller particles such as 5 and 10 nm is the coagulation that occurs after the silica coating is on its surface. This effect was reduced by final dilution using ethanol but still could not produce large percentage of single particles. The

possible causes for coagulation though not detected should be studied more comprehensively. Some of the causes mentioned are hydrogen bonding, drying effect on grid or insufficient surface charge on silica. Though other attempts were made to prevent coagulation, the results were not much different and thus coagulation still existed.

Optical experiments gave expected results for both bare and silica coated gold. The film preparation technique gave better results and shows increase in absorbance value and red shift towards the solution peak spectra with each consecutive layer. In addition, there is a red shift of silica coated gold particle with respect to bare gold spectra that matches previous results of various authors [3,18]. Finally, the aggregates formed while forming film of bare gold particles proves the fact that silica coating is required to form stabilized gold film and thus functional composite structures.

APPENDIX A.

ABSORPTION SPECTROMETER

The absorption spectrometer used for the absorption experiments is made by Ocean Optics Inc.; FL with model number USB 2000 is a miniature fiber optic spectrometer. The general setup of this spectrometer is as shown in Figure A.1. The light source available for absorption experiments is both in UV and Visible range i.e. from 200 nm to 850 nm. It can also perform transmission, reflectance and emission experiments using this spectrometer. The major advantage is the immediate readings displayed on the computer while performing the experiments. Also the software included with it helps in analyzing the absorbance data.

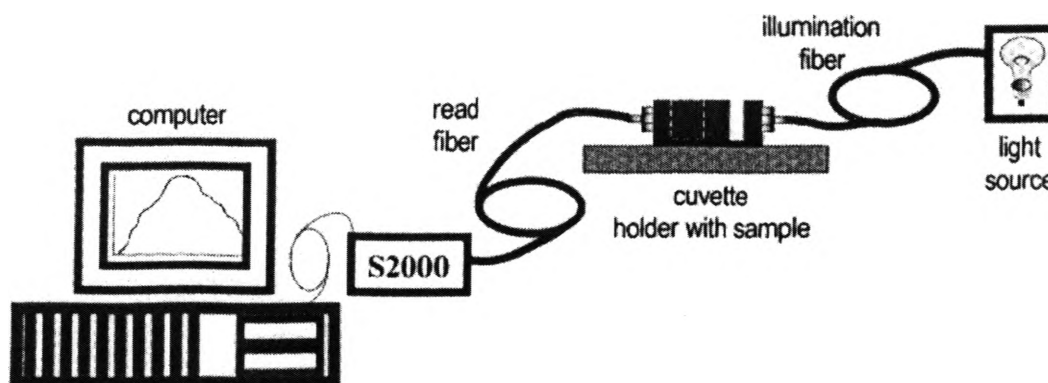


Figure A.1. Experimental set-up of fiber optic spectrometer.

The exploded diagram of cuvette holder is as per Figure A.2 below. The sample is placed in the slot provided in such a way as to let the light pass through it without any obstacle.

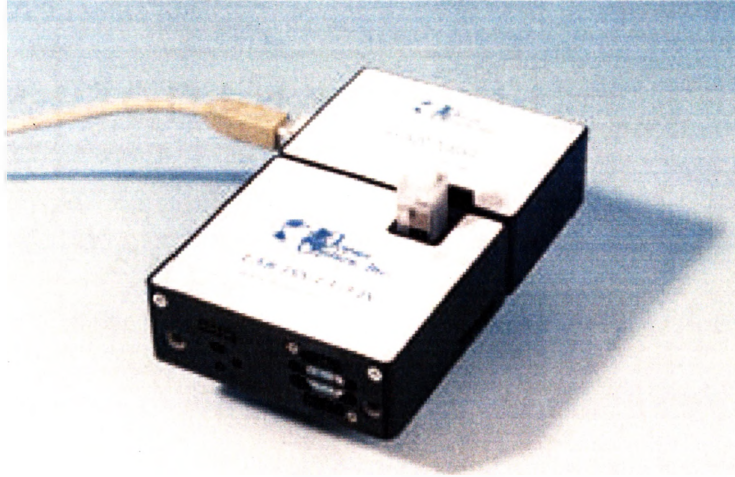


Figure A.2. Exploded view of the cuvette.

APPENDIX B.

TRANSMISSION ELECTRON MICROSCOPE

A Transmission Electron Microscope (TEM) is used to determine the internal structure of materials, either biological or non-biological origin. The basic operation of TEM is based on the phenomenon of passing a high energy electron beam through the sample which absorbs and scatters electrons to form a magnified image. This magnified image can be seen visibly after the electron intensity is transformed to visible light intensity for analysis. The resolution of the TEM dictates the magnification that can be achieved to view the sample. As a rule of thumb a high resolution TEM operating at 300 kV is enough to view 2 nm nanoparticles easily. Figure B.1 below shows a general TEM set-up. It has a cylindrical chamber through which electrons pass through the sample.

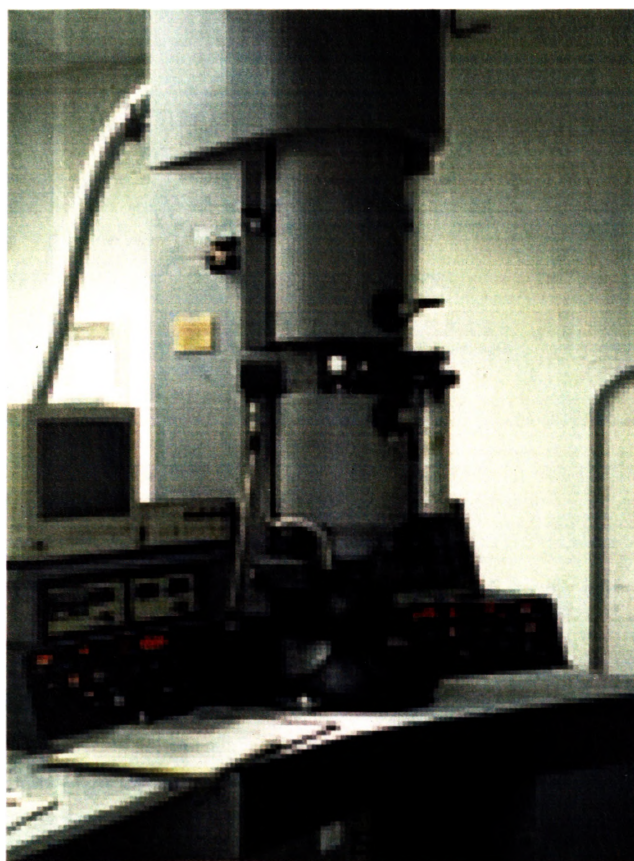


Figure B.1. Transmission electron microscope.

This chamber is cooled by liquid nitrogen at all times to prevent overheating. Also the chamber is in vacuum condition when electron beams passes through it. The magnified image of the sample can be seen through the fluorescent window present at the bottom of the chamber. The sample preparation for TEM is important for a good image. The sample or the TEM grid should be thin enough to let the electrons transmit through it efficiently. In addition to size and shape of the nanoparticle, qualitative analysis can also be done using TEM.

BIBLIOGRAPHY

1. Frank, C. (2001) Nanoengineering of Particle Surfaces. *Advanced Materials* **13(1)** 11-22.
2. Simon, R.H., Sean, A.D. and Stephen, M. (2000) Cocondensation of Organosilica Hybrid Shells on Nanoparticle Templates: A direct Synthetic Route to Functionalized Core-Shell Colloids. *Langmuir* **16** 1454-1456.
3. Nalwa, H.S. (2001) *Handbook of Surfaces and Interfaces of Materials* Volume 3, Academic Press.
4. Stöber, W. and Fink, A. (1968) Controlled Growth of Monodisperse Silica Spheres in the Micron Size Range *Journal of Colloid and Interface Science* **26** 62-69.
5. Liz-Marzán, L.M., Giersig, M. and Mulaveny, P. (1996) Synthesis of Nanosized Gold-Silica Core Shell-Particles. *Langmuir* **12** 4329-4335.
6. Liz-Marzán, L.M. and Philipse, A.P. (1995) Synthesis and optical properties of gold-labeled silica particles. *Journal of Colloid and Interface Science* **176(2)** 459-466.
7. Brinker, C.J. (1988) Hydrolysis and Condensation of Silicates: Effects on structure. *Journal of Non-Crystalline Solids* **100** 31-50.
8. Harris, M.T., Brunson, R.R. and Byers, C.H. (1990) The Base-Catalyzed Hydrolysis and Condensation Reactions of Dilute and Concentrated TEOS Solutions. *Journal of Non-Crystalline Solids* **121** 397-403.
9. Bergna, E.H. (1990) *The Colloid Chemistry of Silica* Advances in Chemistry Series 234 American Chemical Society, Washington D.C.
10. Chen, S.L., Dong, P., Yang, G.H. and Yang, J.J. (1996) Kinetics of Formation of Monodisperse Colloidal Silica Particles through the Hydrolysis and Condensation of Tetraethylorthosilicate *Industrial and Engineering Chemistry Research* **35(12)** 4487-4493.
11. Bogush, G.H. and Zukoski, C.F. (1990) Uniform Silica Particle Precipitation: An Aggregative Growth Model. *Journal of Colloid and Interface Science* **142(1)** 19-34.
12. Bogush, G.H. and Zukoski, C.F. (1990) Studies of the Kinetics of the Preparation of uniform Silica Particles through the Hydrolysis and Condensation of Silicon Alkoxides. *Journal of Colloid and Interface Science* **142(1)** 1-18.
13. Iler, R.K. (1979) *The Chemistry of Silica* Wiley, New York.

14. Allen, L.H. and Matijevic, E. (1969) Stability of colloidal silica. I. Effect of simple electrolytes. *Journal of Colloid and Interface Science* **31(5)** 287-296.
15. Turkevich, J., Stevenson, P.C. and Hiller, J. (1951) A Study of the Nucleation and Growth Processes in the Synthesis of Colloidal Gold. *Discussions of the Faraday Society* **11** 55-75.
16. Epameinondas, L., Konstantina, K., Tasoula, K.L., Vlasoula, B. and Panagiotis, L. (2002) Gold Colloids from Cationic Surfactant Solutions. 1. Mechanisms That Control Particle Morphology *Langmuir* **18** 3659-3668.
17. Plueddermann, E.P. (1991) *Silane Coupling Agents* Plenum, New York.
18. Robert, I.N., Dhanasekran, T., Yimei, C., Robert, J. and Agnes, E.O. (2002) Self-Assembled Highly Ordered Spherical Mesoporous Silica / Gold Nanocomposites. *Advanced Materials* **14(7)** 529-532.
19. Bird, P.G. (1940) US Patent No. 2,244,325.
20. Thearith, U., Liz-Marzán, L.M. and Paul, M. (2001) Optical Properties of Thin Films of Au @ SiO₂ Particles. *Journal of Physical Chemistry B* **105** 3441-3452.
21. Milligan, W.O. and Morris, R.H. (1964) Morphology of Colloidal Gold-A Comparative Study *Journal of the American Chemical Society* **86(17)** 3461-3467.
22. Dirk, G.K. and Thomas, B. (1993) Surface Reactions on thin Layers of Silane Coupling Agents. *Langmuir* **9** 2965-2973.

VITA

Milind Laxman Surve was born on July 26, 1979 in Mumbai, India. He completed his schooling in Mumbai. In 1996 he joined University of Mumbai, India for his B.E. in Chemical Engineering. After completing his undergraduate degree in June 2000, he joined the University of Missouri-Rolla, Rolla, Missouri, in 2001 for his M.S. in Chemical Engineering under Dr. Yangchuan Xing. He received his master's degree in August 2003.